



Supporting Online Material for

Deep-Sea Oil Plume Enriches Indigenous Oil-Degrading Bacteria

Terry C. Hazen,* Eric A. Dubinsky, Todd Z. DeSantis, Gary L. Andersen, Yvette M. Piceno, Navjeet Singh, Janet K. Jansson, Alexander Probst, Sharon E. Borglin, Julian L. Fortney, William T. Stringfellow, Markus Bill, Mark S. Conrad, Lauren M. Tom, Krystle L. Chavarria, Thana R. Alusi, Regina Lamendella, Dominique C. Joyner, Chelsea Spier Jacob Baelum, Manfred Auer, Marcin L. Zemla, Romy Chakraborty, Eric L. Sonnenthal, Patrik D'haeseleer, Hoi-Ying N. Holman, Shariff Osman, Zhenmei Lu, Joy D. Van Nostrand, Ye Deng, Jizhong Zhou, Olivia U. Mason

*To whom correspondence should be addressed. E-mail: tchazen@lbl.gov

Published 24 August 2010 on *Science Express*
DOI: 10.1126/science.1195979

This PDF file includes:

Methods
Figs. S1 to S18
Tables S1 to S8
References

Title: **Deep-sea oil plume enriches indigenous oil-degrading bacteria**

Supplemental Material

Supplemental Data

The LBNL Mississippi Canyon (MC) 252 oil leak Wiki

(http://vimss.lbl.gov/horizonwiki/index.php/Main_Page) has all protocols used and samples collected for each mission for each ship including maps with sample locations for each mission.

Methods

Sample Collection

Water samples were collected from the Gulf of Mexico during two monitoring cruises from May 27-June 2 on the R/V Ocean Veritas and R/V Brooks McCall. The cruises were conducted as part of the monitoring effort to assess the effect of subsea dispersant use during the MC252 oil leak (<http://www.epa.gov/bpspill/dispersants.html#directives>). A colored dissolved organic matter (CDOM) WETstar fluorometer (WET Labs, Philomath, OR) was attached to a CTD sampling rosette (Sea-Bird Electronics Inc., Bellevue, WA) and used to detect the presence of oil along depth profiles between the surface and seafloor. Fluorometer results were subsequently confirmed with laboratory hydrocarbon analysis. A total of seventeen samples were analyzed from ten locations (Fig. S1).

Niskin bottles attached to the CTD rosette were used to capture water samples at various depths inside and outside waters with detected hydrocarbons. The Niskin bottles were cleaned internally with distilled water and detergents between samplings. The sampling crews were sensitive to the problem of contamination from surface oil and used physical methods to disperse

the surface slick before initiating sampling by the CTD, e.g. prop wash at the back of the ship before deployment and recovery, and detergent if prop wash was insufficient. For side deployments the surface of the water was sprayed with freshwater to disperse surface oil, if this was insufficient detergent was applied to the surface of the water then sprayed with freshwater to disperse surface oil. From each sample 800-2000 ml of water was filtered through sterile filter units containing 47 mm diameter polyethylenesulfone membranes with 0.22 μm pore size (MO BIO Laboratories, Inc., Carlsbad, CA) and then immediately frozen and stored at -20°C for the remainder of the cruise. Filters were shipped on dry ice to Lawrence Berkeley National Laboratory and stored at -80°C until DNA and PLFA extraction.

100 ml of water was syringe-filtered and injected into pre-evacuated 125 ml serum bottles capped with thick butyl rubber stoppers. 100 ml of water was frozen in 125 ml HDPE bottles for nutrient analyses. For AODC 36 ml water was preserved in 4% formaldehyde (final concentration).

Fixed Wavelength Fluorescence Analysis (Ship Based)

Two fixed wavelength UV fluorometers (Quantech/Thermo Scientific) were employed in tandem to determine fluorescence intensity ratios (FIRs). One fluorometer was equipped with a pair of wavelength filters allowing excitation at 280 nm and emission at 340 nm. The second fluorometer was equipped with the same 280nm excitation filter and a longer (445 nm) wavelength. Two individual aliquots of 3 ml were transferred to either methacrylate or UV grade quartz cuvettes, and emission at 340 nm and 445 nm was recorded on the respective fluorometers. FIRs were then calculated from fluorescence intensity at 340 nm divided by intensity at 445 nm.

Synchrotron Radiation-based Fourier Transform Infrared (SR-FTIR) spectromicroscopy

SR-FTIR spectroscopy is capable of detecting and differentiating amongst petroleum products, petroleum degradation products, as well as macromolecules of biological samples. The spatial resolution of SR-FTIR, coupled with optical microscopy, is diffraction limited, or between 2 and 10 micrometers in the mid-infrared, and with a signal-to-noise ratio 100-1000 times better than the conventional FTIR method(S2). SR-FTIR analyses were conducted on fresh samples. The location of the synchrotron probe relative to targets selected with optical microscopy was calibrated using infrared-sensitive targets on standards. Excessive seawater was removed prior to SR-FTIR measurements. Background spectra were obtained and used as reference spectra for both samples and standards to remove background H₂O and CO₂ absorptions.

Phospholipid Fatty Acid analysis (PLFA) method

Filters collected in the field were extracted by the Bligh-Dyer method(S3-S5). Briefly, filters were added to 10 ml of a 10:5:4 mixture of methanol:chloroform:pH 7 phosphate buffer to which 50µL of 500 mg/L 1,2-dinonadecanoyl-sn-glycero-3-phosphocholine (Avanti Polar Lipids, Alabaster, Alabama) was added as an internal standard. The mixture was vortexed, sonicated for 2 min and extracted at room temperature in the dark for at least 3 h. Phases were separated with the addition of 5 ml of chloroform and 5 ml of water, vortexed, and centrifuged at 2000 rpm for 15 minutes to separate the organic and aqueous layers. The lower organic layer was removed to a clean tube and 5 ml additional chloroform was added to the original extract which was re-vortexed and centrifuged and combined with the first layer. This combined organic layer was

dried under N₂. The dried extracts were separated into neutral, glycerol, and phospholipids on a C-18 silica column by sequential elution with chloroform, acetone, and methanol. All collected fractions were dried under N₂.

The methanol fraction which contain phospholipids were subjected to a mild alkaline hydrolysis to remove the head group and create fatty acid methyl esters (FAME) compounds. The dried extracts were resuspended with 1:1 chloroform:methanol and 1 ml of 11.2 mg/L KOH in methanol. After vortexing for 2 min they were incubated in a water bath at 37°C for 60 min. The resulting FAME compounds were neutralized with 200 µL of 0.1 mM acetic acid, extracted with 3x2ml of hexane, and dried under N₂. 50 µL of 46.2 mg/L methyl undecanoate (Sigma Chemicals, St. Louis, MO) was added to the dried extracts as an external standard. FAME were detected on an Agilent 6890N GC/FID on a HP1 60m column x 0.25 mm ID and quantified by comparing to known standards. Peak confirmation was accomplished by Agilent 6890 GC/MS. Double bond position was confirmed by DMDS derivatization(S6).

Nutrient Analyses

Total ammonia nitrogen (TAN), was quantified using the TL-2800 ammonia analyzer made by Timberline Instruments (Boulder, CO)(S7). Nitrite (NO₂-N) was measured colormetrically using SM 4500-NO₂-N. Total Iron (Tot Fe) was measured using a reaction with phenanthroline according to SM 3500-Fe B. Ortho-phosphate (PO₄-P) was quantified on unfiltered samples by the ascorbic acid method adapted from SM 4500-P-E(S8).

Acridine Orange Direct Counts

Samples for direct counts were preserved with 4% formaldehyde and stored at 4°C. 1 to 10 ml sample were filtered through a 0.2 µm pore size black polycarbonate membrane (Whatman International Ltd., Piscataway, NJ) supported by a vacuum filtration sampling manifold (Millipore Corp., Billerica, MA). Filtered cells were stained with 25 mg/ml acridine orange for 2 min in the dark. Unbound acridine orange was filtered through the membrane with 10 ml filter sterilized 1X PBS (Sigma Aldrich Corp., St. Louis, MI) and the rinsed membrane was mounted on a slide for microscopy. Cells were imaged with a FITC filter on a Zeiss Axioskop (Carl Zeiss, Inc., Germany)(S9).

SEM methods

For scanning electron microscope imaging, aliquots of fixed samples were passed through 0.2 µm Millipore filter membranes. The filters were then gently rinsed two times in 0.1M sodium cacodylate buffer for 15 minutes and post-fixed using 1% osmium tetroxide in 0.1M sodium cacodylate buffer for an hour and a half at room temperature. Filters were then dehydrated for 10 minutes at each step of a graded ethanol series (20%, 35%, 50%, 75%, 95%, 100%) and critical point dried using a Tousimis AutoSamdri 815 Critical Point Dryer (Tousimis, Rockville, MD). The filters were then sputter-coated with a 20-25nm layer of gold/palladium using a BioRad E5400 Sputter Coater (BioRad, Hercules, CA). Images were collected using a Hitachi S-5000 Scanning Electron Microscope (Hitachi High Technologies America, Inc. Pleasanton, CA).

Petroleum hydrocarbon Methods

To determine hydrocarbon concentrations derived from the presence of oil in the samples, 200 μL of chloroform was added to the neutral lipid extract which was then vortexed followed by a 30 second sonication. The extract was analyzed on an Agilent GC/FID and peaks were identified by GC/MS. Quantification was accomplished by comparison to a known hexadecane standard. Volatile aromatic hydrocarbons were measured using USEPA methods 5030/8260b using an Agilent 6890 GC with 5973 mass spectrometer detector. Initial oven temperature 10°C , initial time 3.00 min, ramp $8^{\circ}\text{C}/\text{min}$ to 188°C , then $16^{\circ}\text{C}/\text{min}$ to 220°C , hold for 9.00 min. Split ratio 25:1. Restek Rtx-VMS capillary column, 60 meter length by 250 micron diameter, 1.40 micron film. Scan 50 to 550 m/z.

DNA Extraction

Filters were extracted using a modified Miller method(S10). One quarter of each filter was cut into small pieces and placed in a Lysing Matrix E tube (MP Biomedicals, Solon, OH). 300 μL of Miller phosphate buffer and 300 μL of Miller SDS lysis buffer were added and mixed. 600 μL phenol:chloroform:isoamyl alcohol (25:24:1) was then added, and the tubes were bead-beat at 5.5m/s for 45sec in a FastPrep instrument. The tubes were spun at 16,000 x g for 5 min at 4°C . 540 μL of supernatant was transferred to a 2 ml tube and an equal volume of chloroform was added. Tubes were mixed and then spun at 10,000 x g for 5 min 400 μL aqueous phase was transferred to another tube and 2 volumes of Solution S3 (MoBio, Carlsbad, CA) was added and mixed by inversion. The rest of the clean-up procedures followed the instructions in the MoBio Soil DNA extraction kit. Samples were recovered in 60 μL Solution S5 and stored at -20°C .

Polymerase Chain Reaction

The 16S rRNA gene was amplified using PCR with primers 27F (5'-AGAGTTTGATCCTGGCTCAG-3') and 1492R (5'-GGTTACCTTGTTACGACTT-3') for bacteria and 4Fa (5'-TCCGGTTGATCCTGCCRG-3') and 1492R for archaea. Each PCR reaction contained 1× Ex Taq buffer (Takara Bio Inc., Japan), 0.025 units/μl Ex Taq polymerase, 0.8 mM dNTP mixture, 1.0 μg/μl BSA, and 200 pM each primer and 0.15-0.5 ng genomic DNA as template. For the PhyloChip assay (PhyloTech Inc. San Francisco, CA) analysis each sample was amplified in 4 replicate 25 μl reactions spanning a range of annealing temperatures. PCR conditions were 95°C (3 min), followed by 30 cycles 95°C (30 s), 46-56°C (25 s), 72°C (2 min), followed by a final extension 72°C (10 min). Amplicons from each reaction were pooled for each sample, purified with the QIAquick PCR purification kit (Qiagen, Valencia, CA), and eluted in 20 μL elution buffer.

Construction of clone libraries

Bacterial 16S rRNA genes were PCR amplified using the primer set B27F and 1492R for 30 cycles. Three clone libraries from samples BM580104, OV00301, and OV01102/03 were generated by ligating 16S amplicons into the pCR4-TOPO cloning vectors (Invitrogen). 96 clones from each library were selected. Inserts were PCR amplified and sequenced bi-directionally using M13F and M13R primers.

Sequence analysis

Plasmid vectors were trimmed, contigs were generated, and sequence quality (chimeras) was checked using GreenGenes (<http://greengenes.lbl.gov/>). This analysis resulted in 250 high

quality sequences, which were used for construction of a distance matrix with greengenes. The DOTUR-1.53 program (S11) was applied to cluster sequences into operational taxonomic units (OTUs) based on 97.5% sequence similarity (S12-S14). Final trees were computed in ARB software package (S15) based on the neighbour joining algorithm with bootstrap values of 1000 replicates.

PhyloChip Assay Design

The PhyloChip microarray probe design approach previously described(S16) was extended and re-applied to all known high-quality 16S rRNA gene sequences containing at least 1,300 nucleotides. Briefly, sequences (*Escherichia coli* base pair positions 47 to 1473) were extracted from the NAST multiple sequence alignment(S17) available from the 16S rRNA gene database, greengenes.lbl.gov(S18). This region was selected because it is flanked by universally conserved segments that can be used as PCR priming sites to amplify bacterial or archaeal genomic material using only 2 to 4 primers(S19). Putative chimeric sequences were identified and removed where Bellerophon (S20) divergence ratios ≥ 1.1 with $\geq 90\%$ lane-masked identity to one or both putative parents were encountered. Sequences containing three or greater homooctomers or longer or those with $\geq 0.3\%$ ambiguous base calls were also omitted. From the sub-alignment, putative 25 mer targets were selected with G+C of content ranging from 35-75%, secondary structure free energy (ΔG) ≥ -4 kcal/mol as calculated by RNAfold(S21), complementary melting temperature of 61°C and 80°C, and self-dimerization melting temperature less than 35°C as calculated by Thermalign (S22).

Filtered rRNA gene sequences were clustered to enable selection of perfectly complementary probes representing each sequence of a cluster. Putative amplicons containing

17-mers with sequence identity to a cluster were included in that cluster. The resulting 59,959 clusters, each encapsulating an average of 0.5% sequence divergence (Fig S12), were considered operational taxonomic units (OTUs). The OTUs represented 2 domains, 147 phyla, 1,123 classes, and 1,219 orders demarcated within the archaea and bacteria. Each OTU was assigned to one of 1,464 families according to the placement of its member organisms in the taxonomic outline as maintained by Philip Hugenholtz (S23). The OTUs comprising each family were clustered into sub-families by transitive (single linkage) sequence identity of 72% common heptamers. Altogether, 10,993 sub-families were found.

The objective of the probe selection strategy was to obtain an effective set of probes capable of correctly categorizing mixed amplicons into their proper OTU. For each OTU, multiple specific 25-mer targets were sought for prevalence in members of a given OTU but dissimilar from sequences outside the given OTU. In the first step of probe selection for a particular OTU, each of the sequences in the OTU was separated into overlapping 25-mers, the potential targets. Then each potential target was matched to as many sequences of the OTU as possible. It was not adequate to use simplistic pattern searches to match potential targets and sequences since partial gene sequences were included in the reference set. Therefore, the multiple sequence alignment provided by Greengenes was necessary to provide a discrete measurement of group size at each potential probe site. For example, if an OTU containing seven sequences possessed a probe site where one member was missing data, then the site-specific OTU size was only six. In ranking the possible targets, those having data for all members of that OTU were preferred over those found only in a fraction of the OTU members. In the second step, a subset of the prevalent targets was selected and the probe orientation was flipped to the reverse complement to minimize hybridization to unintended amplicon. Probes

presumed to be potentially problematic were 25-mers containing a central 17-mer matching sequences in more than one OTU(S24). Thus, probes that were unique to an OTU solely due to a distinctive base in one of the four flanking bases were avoided. Also, probes with mis-hybridization potential to sequences having a common tree node near the root were favored over those with a common node near the terminal branch. Probes complementary to target sequences that were selected for fabrication are termed perfectly matching (PM) probes. As each PM probe was chosen, it was paired with a control 25-mer (mismatching probe, MM), identical in all positions except the thirteenth base. The MM probe did not contain a central 17-mer complementary to sequences in any OTU. The probe complementing the target PM and MM probes constitute a probe pair analyzed together. The average number of probe pairs assigned to each OTU was 37 (s.d. 9.6).

The chosen oligonucleotides were synthesized by a photolithographic method at Affymetrix Inc. (Santa Clara, CA) directly onto a glass surface at an approximate density of 10,000 molecules per μm^2 (S25) and placed into “midi 100 format” hybridization cartridges. The entire array of 1,016,064 probe features was arranged as a grid of 1,008 rows and columns. Of these features, the majority represents publicly available 16S rRNA genes, as described above. Additional probes for quality management, processing controls, image orientation, normalization controls, hierarchical taxonomic identification, or for pathogen-specific signature (S26) detection and some implement additional targeted regions of the chromosome (S27). Furthermore, probes complementary to lower confidence 16S sequences were included to enable broadening the phylogenetic scope of analysis, when those sequences are validated with unambiguous entries into public repositories. The PhyloChip assay design includes control probes for preanalytic, processing, pre-labeled hybridization controls, and negative controls.

Preanalytic and hybridization controls also interpretation of background signal intensity and support normalization of overall fluorescent intensity for sample to sample comparisons.

Preparation of Samples for PhyloChip Assays

From Deep Horizon nucleic acids, 500 ng of bacterial PCR product and 25 ng of archaeal PCR product were prepared for PhyloChip hybridization. PCR mass of the Latin Square samples is listed in Table S8. PCR products were fragmented (S28, S29) to a range of 50-200 bp as verified by agarose gels. Commercial kits were utilized for DNA preparation: Affymetrix (Santa Clara, CA) WT Double Stranded DNA Terminal Labeling, and Affymetrix GeneChip Hybridization, Wash, and Stain kits were used for PhyloChip analysis. Briefly, fragmented 16S amplicons and non-16S quantitative amplicon reference controls were labeled with biotin in 40 μ L reactions containing: 8 μ L of 5X TDF buffer, 40 units of TDF, 3.32 nanomoles of GeneChip labeling reagent. After incubating at 37°C for 60 min, 2 μ L of 0.5M EDTA was added to terminate the reaction. Labeled DNA was combined with 65 μ L of 2X MES hybridization buffer, 20.4 μ L of DMSO, 2 μ L of Affymetrix control oligo B2, and 0.4 μ L nuclease free water. Each reaction mixture was injected into the hybridization chamber of an array cartridge and incubated for 16 h in an Affymetrix hybridization oven at 48°C and 60 RPM. Hybridization solution was removed and the microarrays were stained and scanned according to the manufacturers instructions.

PhyloChip Assay Analysis

Fluorescent images were captured with the GeneChip Scanner 3000 7G (Affymetrix, Santa Clara, CA). An individual array feature occupied approximately 8x8 pixels in the image

file corresponding to a single probe 25mer on the surface. The central 9 pixels were ranked by intensity and the 75% percentile was used as the summary intensity for the feature. Probe intensities were background-subtracted and scaled to the Quantitative Standards (non-16S spike-ins) and outliers were identified as previously described(S16). The hybridization score (HybScore) for an OTU was calculated as the mean intensity of the perfectly matching probes exclusive of the maximum and minimum.

Comparison of the PM and corresponding MM intensities is summarized as the pair difference score, d :

$$d = 1 - \left(\frac{PM - MM}{PM + MM} \right)$$

The d scores are standardized to enable comparison of probe pairs with various nucleotide compositions. The goal in this transformation is determining if a pair's d value is more similar to d values derived from negative controls (NC, probe pairs without potential cross-hybridization to any 16S rRNA sequence nor Quantitative Standards) or to d values from positive controls which are the Quantitative Standards (QS, probe pairs with PM's matching the non-16S rRNA genes which are spiked into the experiment). Because the d_{QS} values are dependent on their target's A+T count and T count, the QS pairs are grouped by these attributes into classes and a separate distribution of d_{QS} values are found for each. The d_{NC} values are grouped in the same way. A distribution is estimated for each class from the observations. Examples are shown in Figure S13. Comparison of the two orange density plots demonstrate that although both are normally distributed, d_{NC} values are not the same among classes. In class "9T 14AT", the mean d_{NC} is greater than class "4T 11AT", also the variance is greater for class "9T 14AT". Comparing the green density plots (estimated to follow a gamma distribution), quantitative reference controls

for class “4T 11AT” nearly always produce d scores close to zero whereas class “9T 14AT” contains more observations of higher d scores (less distinction between PM and MM). In this example it can be seen that class “9T 14AT” has a larger range of d scores shared by both NC and QS. Each d value from an OTU probe set is compared to the distributions of d_{QS} and d_{NC} from the same class to produce a pair response score, r .

$$r = \left(\frac{pdf_{\gamma}(X = d)}{pdf_{\gamma}(X = d) + pdf_{norm}(X = d)} \right)$$

where :

r = response score to measure the potential that the probe pair is responding to a target and not the background

$pdf_{\gamma}(X = d)_{\gamma}$ = probability that d could be drawn from the gamma distribution estimated for the target class ATx Ty

$pdf_{norm}(X = d)_{\gamma}$ = probability that d could be drawn from the normal distribution estimated for the target class ATx Ty

The r scores for a set of probe pairs complimentary to an OTU are considered collectively in Stage 1 probe set Presence/Absence scoring. At minimum, 18 probe pairs are considered. The r scores are ranked and the quartiles, rQ_1 , rQ_2 and rQ_3 are found. For an OTU to pass Stage 1, all three of the following criteria must be met: $rQ_1 \geq .70$, $rQ_2 \geq 0.95$, and $rQ_3 \geq 0.98$. OTUs which pass Stage 1 are considered in Stage 2 scoring for subfamily detection. In this stage, a cross-hybridization adjusted response score, r_x , is calculated for all responsive probes ($r > 0.5$):

$$r_x = \frac{r_i}{\text{scalar}(O_{S1} \cap O_h)}$$

where :

O_{S1} = the set of subfamilies with OTUs passing Stage 1

O_h = the set of subfamilies containing sequences with putative ability to hybridize to PM probe

$\text{scalar}(O_{S1} \cap O_h)$ = the count of subfamilies with hybridization potential and passing Stage 1

After all penalties are considered, the r_x values are ranked and quartiles found as above (r_xQ_1 , r_xQ_2 , r_xQ_3). Subfamilies having a r_xQ_3 values ≥ 0.48 were considered present.

Significantly enriched OTUs within the plume were defined as those achieving a p-value < 0.05 with Student's t-test upon \log_2 (HybScores), Stage1 present call in ≥ 4 of 9 plume samples, and an increase in mean HybScores compared to background (outside of plume samples) of > 1000 units and $> 35\%$.

PhyloChip Assay Performance

Twenty-six 16S rDNA mixtures from different species were prepared as mock communities using a semi-randomized Latin square structure described by Jacobson and Mathews(S30). A stepwise function was used so that each successive organism was added at a final concentration 37% greater than the previous organism. Each test organism was represented in all mixtures at each possible concentration step (Table S8). The 26 DNA mixtures were hybridized in triplicate on different days. Also as a control, one hybridization was carried out using d only to the quantitative reference controls. All 16S probe pairs producing a response score, r , above 0.5 for the reference controls were masked from subsequent analysis.

Background-subtracted probe intensities from 12,202 replicate probes representing 3,548 different 25-mer combinations were used to determine the coefficient of variation (CV) for each assay. Figure S14 displays the CV grouped by mix where each mix was analyzed in 3 different PhyloChip hybridizations on different days. Overall, the variations were minor producing a mean CV = 0.097. Additionally, a significant correlation was found between the concentrations

of each gene in the Latin Square and the corresponding HybScore generating and average correlation coefficient, $r = 0.941$) (Figure S15).

The ability to detect and classify amplicons within the hybridization mix was evaluated using receiver operating characteristic (ROC) curves. The rQ_1 , rQ_2 and rQ_3 probe set summarizations were collected from each of the possible OTUs from all Latin Square results. ROC curves were plotted (Figure S16) to evaluate the effect of choosing a single threshold to determine presence. The y-axis, Expected Positive Rate, is the fraction of OTUs expected to be present that were called present. The x-axis, Unexpected Positive Rate, is the fraction of OTUs not-expected to present that were called present. Presence/Absence thresholds for each quartile were varied from 0, least stringent to 1, most stringent. For example, in the rQ_1 plot, a threshold of 0.5 (green section of curve) allows 97.5% of the expected detection events to pass. Instead of relying on a single threshold to determine presence, all three quartiles of a probe set are examined to ensure the distribution of response scores are skewed toward 1. Collectively, $rQ_1 \geq .70$, $rQ_2 \geq 0.95$, and $rQ_3 \geq 0.98$ was required to achieve a 0.961 Expected Positive OTU Rate for amplicons >2 and <348 pM with a 0.020 Unexpected Positive OTU Rate. In Stage 2 r_xQ_3 subfamily thresholds set at 0.48 allowed a 0.969 Expected Positive Subfamily Rate with a corresponding 0.019 Unexpected Positive Subfamily Rate when applied to the Latin Square data over the same concentration range.

Hybridization results were reduced to a community profile from each PhyloChip assay in a format useful for multivariate statistics. OTUs passing Stage 1 within subfamilies passing Stage 2 constituted the community profile. Replicate community profiles of the Latin Square mock communities were compared by ordination. Inter-profile distance was calculated with either the Bray-Curtis or weighted Unifrac method (S31) and resulting distance matrices were

ordinated with non-metric multidimensional scaling(NMDS) (Figure S17). Profiles from each of the 26 mock communities were clearly distinguishable using either distance method. Analysis of variance using either distance matrix (Adonis) (S32) concluded a significant difference among mock-communities ($p < 0.005$).

GeoChip-based functional gene array hybridization

For assessing the impacts of oil plume on microbial community functional structure, a new generation of functional gene array (GeoChip 4.0) (S33, S34) was used (See the web site for more detailed information related to GeoChip technologies and applications, <http://ieg.ou.edu>). GeoChip 4.0 contained 83,992 50 mer oligonucleotide probes targeting 152,414 genes in 410 gene categories for different microbial functional and biogeochemical processes including carbon, nitrogen, phosphorus, and sulfur cycling, energy processing, metal resistance and reduction, organic contaminant degradation, stress responses, antibiotic resistance, bacterial phages and important human pathogens (Table S4). GeoChip 4.0 is the most comprehensive functional gene arrays for analyzing microbial community functional structure. GeoChip 4.0 is synthesized by Nimblegen in their 12-plex format (i.e., 12 arrays per slide).

DNA extracted from within the oil plume and non-plume as described above was used for functional gene array hybridization. Aliquots of DNA (4 μ L) were amplified with the Templiphi kit (GE Healthcare; Piscataway, NJ) using WCAG (whole community genome amplification) (S35) with modifications to increase DNA yield and minimize bias. All samples yielded between 2.8-3.3 μ g amplified DNA. The amplified DNA (2 μ g) was then labeled with Cy-3 using random primers and the Klenow fragment of DNA polymerase I (S35). Labeled DNA was then dried in a SpeedVac (45°C, 45 min; ThermoSavant).

Dried DNA was rehydrated with 2.68 μL sample tracking control (NimbleGen, Madison, WI, USA) to confirm sample identity. The samples were incubated at 50°C for 5 min, vortexed for 30 min, and then centrifuged to collect all liquid at the bottom of the tube. Hybridization buffer (7.32 μL), containing 40% formamide, 25% SSC, 1% SDS, 2% Cy5-labeled common oligo reference standard (CORS) target, and 2.38% Cy3-labeled alignment oligo (NimbleGen) and 2.8% Cy5-labeled common oligonucleotide reference standard (CORS) target (S36) for data normalization, was then added to the samples, vortexed to mix, spun down, incubated at 95°C for 5 min, and then maintained at 42°C until ready for hybridization. CORS probes were placed randomly throughout the array and are used for signal normalization (S36).

For hybridization, an HX12 mixer (Nimblegen) was placed onto the array using Nimblegen's Precision Mixer Alignment Tool (PMAT), and then the array is preheated to 42°C on a Hybridization Station (MAUI, BioMicro Systems, Salt Lake City, UT, USA) for at least 5 min. Samples (6.8 μL) were then loaded onto the array surface and hybridized approximately 16 h with mixing. After hybridization, the arrays were scanned with a laser power of 100%. Low quality of spots was removed prior to statistical analysis as described previously(S33). Mantel test was used to establish the relationships between geochemical parameters and microbial community functional structure as described previously(S37).

Biodegradation Rates of the Oil Plume

To estimate biodegradation rates in the plume, four data sets representing concentrations of C13-C26 n-alkanes were used to investigate degradation of hydrocarbons in the plume. Two of the data sets were field measurements from sites included in this paper: BM57, BM58, BM53, BM54, OV011, OV010. N-alkanes were not detected in any or the other field samples. The first

data set was provided by BP and included analysis of a wide number of compounds from whole water samples, including n-alkanes. This data set is inclusive of all samples with the exception of OV011. The second data set are n-alkanes quantified from the neutral lipid fraction of the PLFA analysis and represents samples collected on a 0.2 µm PES filter. Both of these data sets were taken from the same CTD deployment but analyzed by different labs. The LBNL and the BP data can be accessed in *The LBNL Mississippi Canyon (MC) 252 oil leak Wiki* under ARF 22 revision 4 (ARF Rev4.pdf). The current analytical list includes: VOAs, PAHs, Alkyl PAHs, Dispersants by DAI (propylene glycol and 2-butoxyethanol), Biomarkers (pristine, phytane, hopanes/triterpanes, steranes, and triaromatic steroids). These analyses are currently being performed by Lancaster laboratories. Initially, Louisiana State University (LSU) laboratory in Baton Rouge was being used for UV-Vis analyses. Samples with detected concentrations of TPH were then analyzed. The LSU lab backlog samples were sent to Gulf Coast Analytical in Baton Rouge, Lancaster Laboratories in Lancaster PA for analysis. Subsequent to that the BP samples were sent to Lancaster.

The other two data sets represent 5°C laboratory degradation studies of degradation of source oil in microcosm water collected outside the plume with MC252 oil as the carbon source and isolates from the plume mixed as a consortia with MC252 oil. Microcosms were set up as triplicates using non-contaminated water from plume depth (OV02302) sampled June 6th 2010. 100 ml of the water was placed in 125 ml serum bottles and crude oil (MC252) was added to obtain a concentration of 100 mg/L. Bottles were closed using Teflon coated rubber stoppers and were incubated at 5°C in the dark for 20 days. Samples for analysis of hydrocarbons were taken after 0, 1, 5, and 20 days of incubation in triplicate samples. Oil Degradation in Consortia: 2 ml of oil plume depth water (OV01003) was enriched in 18 ml bicarb buffered minimal marine

medium (S38) amended with 0.05 g bactopectone and 500 μ L MC252 oil. From this enrichment, after four weeks, a transfer was made into fresh minimal marine media with no Carbon source. After incubation for 48 h, this was used as the inoculum for the oil degradation experiment. The experiment was initiated in 45 ml minimal marine medium with 1000 mg/L MC252 oil as the sole carbon source in triplicates at 5°C. Heat killed controls were set up in parallel to account for abiotic loss of oil hydrocarbons. Samples were withdrawn for GC-MS analyses using sterile syringes after well mixing after 0, 2, 5, and 8 days. Degradation rate coefficients and half-life (Table S3, S4) were calculated from the alkane data from these four sources using the 1st order rate equation (S39, S40). For field experiments, BM53, BM54, and OV011 were considered a day 0 sampling point, and BM57, OV010 were considered intermediate points (either 1 or 3 days) and BM58 was considered the final point (either 2 or 5 days), using estimated travel times of 2 – 5 days between the day 0 and final sampling points. This range is the best estimate given recorded ocean currents (http://www.ndbc.noaa.gov/station_page.php?station=42916&unit=M&tz=STN, (S41)).

References

- S1. Z. K. Li *et al.*, Effects of chemical dispersants and mineral fines on crude oil dispersion in a wave tank under breaking waves. *Mar. Pollut. Bull.* **54**, 983 (Jul, 2007).
- S2. H.-Y. N. Holman, M. C. Martin, in *Advances in Agronomy*. (Elsevier, 2006), vol. 90, pp. 79-127.
- S3. J. B. Guckert, C. P. Antworth, P. D. Nichols, D. C. White, Phospholipid, ester-linked fatty-acid profiles as reproducible assays for changes in prokaryotic community structure of estuarine sediments. *FEMS Microbiol. Ecol.* **31**, 147 (1985).
- S4. S. M. Pfiffner *et al.*, Deep Subsurface Microbial Biomass and Community Structure in Witwatersrand Basin Mines. *Geomicrobiology Journal* **23**, 431 (2006).
- S5. D. C. White, D. B. Ringelberg, Signature lipid biomarker analysis. *Techniques in Microbial Ecology*, 255 (1998).
- S6. P. D. Nichols, J. B. Guckert, D. C. White, Determination of Monounsaturated Fatty-Acid Double-Bond Position and Geometry for Microbial Monocultures and Complex

- Consortia by Capillary Gc-Ms of Their Dimethyl Disulfide Adducts. *J. Microbiol. Methods* **5**, 49 (May, 1986).
- S7. R. M. Carlson, R. I. Cabrera, J. L. Paul, J. Quick, R. Y. Evans, Rapid Direct Determination of Ammonium and Nitrate in Soil and Plant-Tissue Extracts. *Commun. Soil Sci. Plant Anal.* **21**, 1519 (1990).
- S8. *Standard Methods of the Examination of Water and Wastewater*. (American Public Health Association, Washington, DC, 2005).
- S9. Francisc.De, R. A. Mah, A. C. Rabin, Acridine Orange-Epifluorescence Technique for Counting Bacteria in Natural Waters. *Transactions of the American Microscopical Society* **92**, 416 (1973).
- S10. D. N. Miller, J. E. Bryant, E. L. Madsen, W. C. Ghiorse, Evaluation and optimization of DNA extraction and purification procedures for soil and sediment samples. *Appl. Environ. Microbiol.* **65**, 4715 (Nov, 1999).
- S11. P. D. Schloss, J. Handelsman, Metagenomics for studying unculturable microorganisms: cutting the Gordian knot. *Genome Biol.* **6**, 4 (2005).
- S12. B. M. Goebel, E. Stackebrandt, Cultural and Phylogenetic Analysis of Mixed Microbial-Populations Found in Natural and Commercial Bioleaching Environments. *Appl. Environ. Microbiol.* **60**, 1614 (May, 1994).
- S13. B. Lawley, S. Ripley, P. Bridge, P. Convey, Molecular analysis of geographic patterns of eukaryotic diversity in Antarctic soils. *Appl. Environ. Microbiol.* **70**, 5963 (Oct, 2004).
- S14. R. Rossello-Mora, R. Amann, The species concept for prokaryotes. *Fems Microbiol. Rev.* **25**, 39 (Jan, 2001).
- S15. W. Ludwig *et al.*, ARB: a software environment for sequence data. *Nucleic Acids Res.* **32**, 1363 (Feb, 2004).
- S16. T. Z. DeSantis *et al.*, High-density universal 16S rRNA microarray analysis reveals broader diversity than typical clone library when sampling the environment. *Microb Ecol* **53**, 371 (Apr, 2007).
- S17. T. Z. DeSantis *et al.*, NAST: a multiple sequence alignment server for comparative analysis of 16S rRNA genes. *Nucleic Acids Res* **34**, W394 (Jul 1, 2006).
- S18. T. Z. DeSantis *et al.*, Greengenes, a chimera-checked 16S rRNA gene database and workbench compatible with ARB. *Appl Environ Microbiol* **72**, 5069 (Jul, 2006).
- S19. M. A. Dojka, P. Hugenholtz, S. K. Haack, N. R. Pace, Microbial diversity in a hydrocarbon- and chlorinated-solvent- contaminated aquifer undergoing intrinsic bioremediation. *Appl Environ Microbiol* **64**, 3869 (1998).
- S20. T. Huber, G. Faulkner, P. Hugenholtz, Bellerophon: a program to detect chimeric sequences in multiple sequence alignments. *Bioinformatics* **20**, 2317 (Sep 22, 2004).
- S21. I. L. Hofacker, Vienna RNA secondary structure server. *Nucleic Acids Res* **31**, 3429 (Jul 1, 2003).
- S22. L. Kaderali, A. Schliep, Selecting signature oligonucleotides to identify organisms using DNA arrays. *Bioinformatics* **18**, 1340 (Oct, 2002).
- S23. P. Hugenholtz, Exploring prokaryotic diversity in the genomic era. *Genome Biol* **3**, 1 (2002).
- S24. H. Urakawa, P. A. Noble, S. El Fantroussi, J. J. Kelly, D. A. Stahl, Single-base-pair discrimination of terminal mismatches by using oligonucleotide microarrays and neural network analyses. *Appl Environ Microbiol* **68**, 235 (2002).

- S25. M. Chee *et al.*, Accessing genetic information with high-density DNA arrays. *Science* **274**, 610 (Oct 25, 1996).
- S26. A. M. Phillippy *et al.*, Comprehensive DNA signature discovery and validation. *PLoS Comput Biol* **3**, e98 (May, 2007).
- S27. W. J. Wilson *et al.*, Sequence-specific identification of 18 pathogenic microorganisms using microarray technology. *Mol Cell Probes* **16**, 119 (2002).
- S28. E. L. Brodie *et al.*, Application of a high-density oligonucleotide microarray approach to study bacterial population dynamics during uranium reduction and reoxidation. *Appl. Environ. Microbiol.* **72**, 6288 (Sep, 2006).
- S29. X. Ge, W. S. Rubinstein, Y. C. Jung, Q. Wu, Genome-wide analysis of antisense transcription with Affymetrix exon array. *BMC Genomics* **9**, 27 (2008).
- S30. M. T. Jacobson, P. Matthews, Generating uniformly distributed random latin squares. *Journal of Combinatorial Designs* **4**, 405 (1995).
- S31. C. Lozupone, R. Knight, UniFrac: a new phylogenetic method for comparing microbial communities. *Appl Environ Microbiol* **71**, 8228 (Dec, 2005).
- S32. M. J. Anderson, A new method for non-parametric multivariate analysis of variance. *Austral Ecology* **26**, 32 (2001).
- S33. Z. He *et al.*, GeoChip 3.0 as a high throughput tool for analyzing microbial community structure, composition, and functional activity. *Isme J.* **doi:10.1038/ismej.2010.46**, 1 (2010).
- S34. Z. L. He *et al.*, GeoChip: a comprehensive microarray for investigating biogeochemical, ecological and environmental processes. *Isme J.* **1**, 67 (May, 2007).
- S35. L. Wu, X. Liu, C. W. Schadt, J. Zhou, Microarray-Based Analysis of Subnanogram Quantities of Microbial Community DNAs by Using Whole-Community Genome Amplification. *Appl. Environ. Microbiol.* **72**, 4931 (July 1, 2006, 2006).
- S36. Y. Liang *et al.*, Development of a Common Oligonucleotide Reference Standard for Microarray Data Normalization and Comparison across Different Microbial Communities. *Appl. Environ. Microbiol.* **76**, 1088 (February 15, 2010, 2010).
- S37. J. Z. Zhou, S. Kang, C. W. Schadt, C. T. Garten, Spatial scaling of functional gene diversity across various microbial taxa. *Proc. Natl. Acad. Sci. U. S. A.* **105**, 7768 (Jun, 2008).
- S38. J. D. Coates, D. J. Lonergan, E. J. P. Philips, H. Jenter, D. R. Lovley, *Desulfuromonas palmitatis* sp nov, a marine dissimilatory Fe[III] reducer that can oxidize long-chain fatty acids. *Arch. Microbiol.* **164**, 406 (Dec, 1995).
- S39. S. J. MacNaughton *et al.*, Microbial Population Changes during Bioremediation of an Experimental Oil Spill. *Appl. Environ. Microbiol.* **65**, 3566 (August 1, 1999, 1999).
- S40. A. D. Venosa, E. L. Holder, Biodegradability of dispersed crude oil at two different temperatures. *Mar. Pollut. Bull.* **54**, 545 (May, 2007).
- S41. P. Hamilton, Deep Currents in the Gulf of Mexico. *J. Phys. Oceanogr.* **20**, 1087 (Jul, 1990).
- S42. O. G. Brakstad, I. Nonstad, L. G. Faksness, P. J. Brandvik, Responses of microbial communities in Arctic sea ice after contamination by crude petroleum oil. *Microbial Ecology* **55**, 540 (2008).
- S43. U. Deppe, H. H. Richnow, W. Michaelis, G. Antranikian, Degradation of crude oil by an arctic microbial consortium. *Extremophiles* **9**, 461 (2005).

- S44. B. Gerdes, R. Brinkmeyer, G. Dieckmann, E. Helmke, Influence of crude oil on changes of bacterial communities in Arctic sea-ice. *FEMS Microbiol. Ecol.* **53**, 129 (Jun, 2005).
- S45. A. Lo Giudice, V. Bruni, M. De Domenico, L. Michaud, in *Handbook of Hydrocarbon and Lipid Microbiology*, K. N. Timmis, Ed. (Springer-Verlag, Heidelberg, 2010), pp. 1897-1921.
- S46. S. M. Powell, J. P. Bowman, I. Snape, Degradation of nonane by bacteria from Antarctic marine sediment. *Polar Biology* **27**, 573 (2004).
- S47. A. Schlosser, A. Lipski, J. Schmalfluss, F. Kugler, G. Beckmann, *Oceaniserpentilla haliotis* gen. nov., sp nov., a marine bacterium isolated from haemolymph serum of blacklip abalone. *Int. J. Syst. Evol. Microbiol.* **58**, 2122 (Sep, 2008).
- S48. Y. N. Wang *et al.*, *Halomonas shengliensis* sp nov., a moderately halophilic, denitrifying, crude-oil-utilizing bacterium. *Int. J. Syst. Evol. Microbiol.* **57**, 1222 (2007).
- S49. M. M. Yakimov *et al.*, Crude oil-induced structural shift of coastal bacterial communities of rod bay (Terra Nova Bay, Ross Sea, Antarctica) and characterization of cultured cold-adapted hydrocarbonoclastic bacteria. *FEMS Microbiol. Ecol.* **49**, 419 (Sep, 2004).
- S50. M. M. Yakimov *et al.*, *Oleispira antarctica* gen. nov., sp nov., a novel hydrocarbonoclastic marine bacterium isolated from Antarctic coastal sea water. *Int. J. Syst. Evol. Microbiol.* **53**, 779 (May, 2003).
- S51. M. M. Yakimov, K. N. Timmis, P. N. Golyshin, Obligate oil-degrading marine bacteria. *Curr. Opin. Biotechnol.* **18**, 257 (Jun, 2007).
- S52. S. Sunagawa *et al.*, Bacterial diversity and White Plague Disease-associated community changes in the Caribbean coral *Montastraea faveolata*. *Isme J.* **3**, 512 (May, 2009).
- S53. G. McGuire, M. C. Denham, D. J. Balding, Models of sequence evolution for DNA sequences containing gaps. *Mol. Biol. Evol.* **18**, 481 (Apr, 2001).

Tables

Table S1. Dispersed MC252 plume and non-plume parameters at 1099-1219 m. Parameter with significant differences are highlighted (Student's T-test, P <0.05)

	Plume mean (s.d.)	Non-Plume mean (s.d.)	T-test p-value (N)
<i>Physical-Chemical</i>			
Fluorescence (mg/m ³)	24.2 (18.2)	5.9 (0.5)	0.018* (17)
Phosphate (μg/L)	39.8 (6.7)	40.7 (4.3)	0.781 (14)
Ammonia-N (μg/L)	23.6 (5.3)	20.8 (2.9)	0.347 (14)
Nitrate-N (μg/L)	277 (80)	359 (99)	0.003** (14)
d13C DIC	-0.57 (0.06)	-0.46 (0.14)	0.174 (10)
<i>Hydrocarbon</i>			
octadecane (ppb)	4.2 (2.4)	0.13 (0.18)	<0.001*** (14)
n-docosane (ppb)	4.7 (2.7)	0.12 (0.17)	<0.001*** (14)
Total volatile aromatic hydrocarb ¹	139 (179)	0.5 (1.8)	<0.001*** (14)
<i>Biological</i>			
Bacteria density (Log(AODC))	4.59 (0.63)	4.01 (0.11)	0.030* (17)
Archaeal_Richness	11 (3)	12 (2)	0.224 (17)
Bacterial_Richness	308 (83)	504 (105)	<0.001*** (17)
Total_Richness	318 (85)	516 (107)	<0.001*** (17)
Log2(Oceanospirillales_clone)	13.6 (0.2)	13 (0.6)	0.013* (17)
Total_PLFA (pm/L)	0.57 (0.31)	0.13 (0.07)	0.002** (16)
PLFA_trans/cis (ratio)	0.21 (0.09)	0.14 (0.03)	0.87 (16)
16:1w5c/16:1w7c (ratio)	14.6 (16.0)	0.6 (1.1)	0.037* (16)

¹ Benzene, toluene, ethylbenzene, isopropylbenzene, n-propylbenzene, 1,3,5-trimethylbenzene, tert-butylbenzene, 1,2,4-trimethylbenzene, sec-butylbenzene, p-isopropyltoluene, n-butylbenzene, naphthalene, o-xylene, m,p-xylenes.

Table S2. γ -proteobacteria taxa enriched by the oil plume. Taxa that include known hydrocarbon degraders or previously shown in cold waters to become enriched in response to crude oil are indicated(S42-51).

Class	Family	Hydrocarbon degraders*	Enriched by crude oil*	Representative sequence
Aeromonadaceae	Aeromonadaceae	+	+	DQ816633.1 Zebrafish gut clone
Alteromonadales	Colwelliaceae	ND	+	EU491914.1 East Pacific Rise deepwater clone AY646431.1
Alteromonadales	Pseudoalteromonadaceae	+	+	<i>Pseudoalteromonas</i> sp. EU544859.1 Arctic seawater clone
Arctic96B-1	Unclassified	ND	+	DQ925906.1 Guaymas Basin clone
BPC036	Unclassified	ND	+	DQ270747.1 <i>Halomonas</i> sp.
Halomonadaceae	Halomonadaceae	+	+	DQ157009.2 <i>Marinobacter haloterrigenus</i>
Marinobacter	Marinobacter	+	+	AF275713.1 <i>Marinospirillum alkaliphilum</i>
Marinospirillum	Marinospirillum	+	+	AF200213.1 Psychrophilic marine isolate
Moraxellaceae	Moraxellaceae	+	+	AY549003.2 Marine bone clone
Oceanospirillales	Marinobacterium	+	+	EF673290.1 <i>Marinomonas</i> sp.
Oceanospirillales	Marinomonas	+	+	AM747817.1 <i>Oceaniserpentilla haliotidis</i>
Oceanospirillales	Unclassified	+	+	AM111047.1 <i>Pseudomonas</i> sp.
Pseudomonadaceae	Pseudomonadaceae	+	+	DQ665797.1 <i>Shewanella frigidimarina</i>
Shewanellaceae	Shewanellaceae	+	+	EU491790.1 East Pacific Rise seafloor clone
Unclassified	Unclassified_sfB	ND	ND	EU652559.1 Yel Sea sediment clone
Unclassified	Unclassified_sfC	ND	ND	

ND = No data

Table S3. Summary of PLFA Data

Sample ID	Date	Sample		Total PLFA cells/ml								
		Depth (m)	Plume	(lipids/ml)	from lipids	unk	14:1	14:0	i14:0	i15:0	a15:0	
OV00301	05/27/10	1020	No	0.222	5.55E+03	0.023	0.000	0.064	0.000	0.000	0.000	0.031
OV00305	05/27/10	300	No	0.094	2.35E+03	0.024	0.000	0.064	0.000	0.000	0.000	0.032
OV00405	05/28/10	1100	No	0.146	3.65E+03	0.022	0.000	0.057	0.000	0.000	0.000	0.029
OV00903	05/29/10	1100	No	0.147	3.67E+03	0.022	0.000	0.057	0.000	0.000	0.000	0.030
OV01001	05/29/10	1155	Yes	0.425	1.06E+04	0.012	0.000	0.027	0.000	0.000	0.000	0.000
OV01003	05/29/10	1135	Yes	0.391	9.78E+03	0.014	0.000	0.029	0.000	0.000	0.000	0.008
OV01005	05/29/10	1100	Yes	0.639	1.60E+04	0.015	0.000	0.019	0.000	0.000	0.000	0.018
OV01101	05/29/10	1285	No	0.639	1.60E+04	0.015	0.000	0.019	0.000	0.000	0.000	0.018
OV01102	05/29/10	1207	Yes	0.165	4.13E+03	0.018	0.000	0.022	0.000	0.000	0.000	0.010
OV01104	05/29/10	1181	Yes	0.722	1.81E+04	0.018	0.000	0.015	0.000	0.000	0.000	0.009
OV01106	05/29/10	1042	No	0.173	4.33E+03	0.013	0.000	0.026	0.000	0.000	0.000	0.012
OV01107	05/29/10	501	No	0.028	6.89E+02	0.028	0.000	0.060	0.000	0.000	0.000	0.000
BM530104	5/30/10	1219	Yes	0.349	8.73E+03	0.013	0.000	0.227	0.000	0.000	0.000	0.000
BM540104	5/30/10	1194	Yes	0.408	1.02E+04	0.024	0.000	0.098	0.000	0.000	0.000	0.000
BM570104	5/31/10	1174	Yes	1.165	2.91E+04	0.035	0.003	0.078	0.002	0.001	0.001	0.012
BM580104	5/31/10	1179	Yes	0.859	2.15E+04	0.032	0.000	0.083	0.000	0.007	0.007	0.025

Sample ID	15:1w10	15:0	i16:0	16:1w5c	16:1w7c	16:0	unk 20.3	i17:1w9c	10Me16:0	a17:1w9c	a17:0
OV00301	0.000	0.035	0.000	0.158	0.019	0.259	0.015	0.009	0.015	0.023	0.025
OV00305	0.000	0.035	0.000	0.139	0.036	0.245	0.000	0.000	0.000	0.049	0.024
OV00405	0.000	0.034	0.000	0.153	0.016	0.247	0.019	0.010	0.015	0.020	0.026
OV00903	0.000	0.033	0.000	0.154	0.014	0.252	0.026	0.000	0.015	0.020	0.026
OV01001	0.000	0.000	0.000	0.110	0.039	0.180	0.000	0.000	0.000	0.000	0.000
OV01003	0.000	0.018	0.000	0.087	0.051	0.171	0.000	0.000	0.000	0.000	0.016
OV01005	0.000	0.023	0.001	0.054	0.161	0.198	0.001	0.067	0.023	0.028	0.027
OV01101	0.000	0.023	0.001	0.054	0.161	0.198	0.001	0.067	0.023	0.028	0.027
OV01102	0.000	0.012	0.004	0.148	0.446	0.115	0.049	0.003	0.005	0.006	0.008
OV01104	0.000	0.014	0.000	0.011	0.237	0.161	0.015	0.000	0.000	0.000	0.016
OV01106	0.000	0.017	0.000	0.096	0.030	0.254	0.023	0.000	0.000	0.039	0.014
OV01107	0.000	0.035	0.000	0.152	0.038	0.281	0.000	0.000	0.000	0.027	0.023
BM530104	0.000	0.000	0.012	0.019	0.089	0.223	0.091	0.000	0.000	0.000	0.000
BM540104	0.000	0.017	0.028	0.013	0.313	0.241	0.031	0.000	0.000	0.000	0.007
BM570104	0.000	0.019	0.019	0.009	0.391	0.190	0.023	0.002	0.003	0.008	0.011
BM580104	0.000	0.033	0.007	0.011	0.352	0.189	0.007	0.000	0.000	0.012	0.021

Sample ID	17cy	17:0	2-OH 16:0	18:3	18:3	18:1w9c	18:1w9t	18:0	unk 27.4	19cy	sat
OV00301	0.000	0.000	0.000	0.000	0.061	0.147	0.016	0.099	0.000	0.000	0.457
OV00305	0.000	0.019	0.000	0.000	0.075	0.146	0.028	0.084	0.000	0.000	0.448
OV00405	0.000	0.017	0.000	0.000	0.066	0.157	0.018	0.093	0.000	0.000	0.449
OV00903	0.000	0.016	0.000	0.000	0.058	0.140	0.016	0.122	0.000	0.000	0.479
OV01001	0.000	0.000	0.000	0.000	0.133	0.321	0.053	0.125	0.000	0.000	0.332
OV01003	0.000	0.009	0.000	0.000	0.210	0.260	0.018	0.097	0.012	0.000	0.323
OV01005	0.000	0.030	0.000	0.000	0.069	0.138	0.030	0.099	0.000	0.000	0.369
OV01101	0.000	0.030	0.000	0.000	0.069	0.138	0.030	0.099	0.000	0.000	0.369
OV01102	0.000	0.008	0.000	0.000	0.022	0.082	0.013	0.028	0.000	0.000	0.186
OV01104	0.000	0.017	0.000	0.000	0.064	0.302	0.043	0.057	0.021	0.000	0.263
OV01106	0.000	0.012	0.000	0.000	0.078	0.155	0.028	0.204	0.000	0.000	0.513
OV01107	0.000	0.000	0.000	0.000	0.060	0.166	0.023	0.108	0.000	0.034	0.484
BM530104	0.000	0.000	0.000	0.000	0.031	0.130	0.023	0.110	0.034	0.000	0.559
BM540104	0.000	0.009	0.000	0.000	0.025	0.097	0.025	0.072	0.000	0.000	0.438
BM570104	0.003	0.009	0.000	0.005	0.034	0.071	0.021	0.044	0.000	0.002	0.340
BM580104	0.007	0.029	0.000	0.005	0.043	0.060	0.023	0.052	0.000	0.001	0.386

Sample ID	mono-unsaturated	branched	brmon	cyc	hyd	unk	cyc/mono	trans/cis	mono/sat	16:1w5c/16:1w7c
OV00301	0.436	0.056	0.048	0.000	0.000	0.039	0.000	0.109	0.953	0.122
OV00305	0.459	0.056	0.049	0.000	0.000	0.024	0.000	0.188	1.025	0.258
OV00405	0.445	0.055	0.045	0.000	0.000	0.040	0.000	0.112	0.991	0.107
OV00903	0.415	0.056	0.035	0.000	0.000	0.048	0.000	0.113	0.866	0.094
OV01001	0.656	0.000	0.000	0.000	0.000	0.012	0.000	0.166	1.975	0.351
OV01003	0.644	0.024	0.000	0.000	0.000	0.026	0.000	0.068	1.993	0.582
OV01005	0.475	0.046	0.117	0.000	0.000	0.016	0.000	0.217	1.288	2.995
OV01101	0.475	0.046	0.117	0.000	0.000	0.016	0.000	0.217	1.288	2.995
OV01102	0.723	0.022	0.014	0.000	0.000	0.067	0.000	0.153	3.887	3.016
OV01104	0.671	0.025	0.000	0.000	0.000	0.054	0.000	0.142	2.550	21.080
OV01106	0.404	0.026	0.039	0.000	0.000	0.035	0.000	0.177	0.789	0.311
OV01107	0.473	0.023	0.027	0.034	0.000	0.028	0.071	0.137	0.976	0.250
BM530104	0.291	0.012	0.000	0.000	0.000	0.138	0.000	0.174	0.520	4.735
BM540104	0.489	0.035	0.000	0.000	0.000	0.055	0.000	0.257	1.119	23.535
BM570104	0.548	0.045	0.013	0.005	0.000	0.066	0.009	0.291	1.614	44.405
BM580104	0.523	0.060	0.012	0.008	0.000	0.040	0.015	0.388	1.355	31.084

Table S4. Summary of GeoChip 4.0 probe and sequence information by functional gene category.

Functional process	Number of gene categories	Number of sequences retrieved	Number of probes designed	Number of CDS covered
Antibiotic resistance	11	15754	3349	5547
Bacterial phages	40	3644	1100	2083
Carbon degradation	33	21529	9033	13667
Carbon fixation	5	5252	1762	3398
Methane metabolism	3	9718	507	1677
Nitrogen cycling	17	47988	7552	17550
Phosphorus utilization	3	3783	1378	2261
Stress responses	45	75305	21574	41033
Sulfur cycling	6	8078	3254	4461
Metal resistance	44	25277	9478	17575
Contaminant degradation	184	44220	17919	30361
Energy process	4	1762	862	1131
Virulence	13	16762	3732	7444
Others (gyrB, bchY)	2	7830	2492	4226
Total	410	286,902	83,992	152,414

Table S5. Mantel test to show the relationships between overall functional community structure and oil contaminants based on the geochemical data from the ten samples (oil contaminated samples: BM053, BM054, BM057, BM058 and BM064; non-oil contaminated samples: OV003, OV004, OV009, OV013 and OV014).

Genes	Environmental variables	Simple mantel	
		<i>r</i>	<i>p</i>
All functional genes	All environmental variables ¹	0.3719	0.022*
	Temperature	0.4147	0.014*
	DO probe	0.3791	0.013*
	Fluorometer detection of oil	0.3289	0.027*
	Small particle concentrations	-0.0571	0.619
	AODC	0.06439	0.323
	Phosphate	-0.084	0.655
	Benzene	0.387	0.017*
	Toluene	0.3868	0.017*
	Isopropylbenzene	0.1633	0.18
	n-Propylbenzene	0.2295	0.086
	1,3,5-Trimethylbenzene	0.176	0.145
	Tert-butylbenzene	0.2186	0.117
	1,2,4-Trimethylbenzene	0.176	0.144
	p-Isopropyltoluene	0.2673	0.069
	n-Butylbenzene	0.2295	0.09
	Naphthalene	0.2973	0.046*
	Total xylenes	0.3759	0.032*
	Total volatile HC	0.3842	0.018*
Total petroleum hydrocarbons - extractable (DRO)	0.1666	0.156	

¹All environmental variables: temperature, DO probe, fluorometer detection of oil, small particle concentrations, AODC, phosphate, benzene, toluene, ethylbenzene, isopropylbenzene, n-propylbenzene, 1,3,5-trimethylbenzene, tert-butylbenzene, 1,2,4-trimethylbenzene, p-isopropyltoluene, n-butylbenzene, naphthalene, total xylenes, total volatile hydrocarbon and total petroleum hydrocarbons - extractable (DRO).

Table S6. Significant relationships ($p < 0.1$) of key hydrocarbon degradation genes to different concentration of oil contaminants. The values in this Table are the p values determined by Mantel test. Any p value < 0.05 is bolded. Only major abundant genes shown here.

Genes	Coded Enzyme	Compound degradation	Number of detected sequences	Dominant Genus	Benzene	Toluene	Isopropyl benzene	n-Propyl benzene	1,3,5-Trimethyl benzene	tert-Butyl benzene	1,2,4-Trimethyl benzene	p-Isopropyl toluene	n-Butyl benzene	Naphthalene
<i>alkI</i>	alcohol dehydrogenase	Dodecyl sulfate	6	<i>Bacillus</i>	0.042	0.03	0.038	0.023			0.031	0.045	0.098	0.039
<i>Arylest</i>	aromatic esterase	Hydroxyacetophenone	30	<i>Burkholderia;</i> <i>Pseudomonas</i>	0.036	0.028			0.052		0.035	0.085		0.055
<i>bbs</i>	E-phenylitaconyl-CoA hydratase	Gallate	2	<i>Aromatoleum;</i> <i>Thauera</i>	0.009	0.019					0.017			0.073
<i>bco</i>	Benzoyl CoA reductase	Benzoate	12	<i>Azoarcus</i>					0.017					
<i>BpH</i>	benzoate 4-monoxygenase	Benzoate	7	<i>Aspergillus</i>	0.065	0.043					0.045	0.099		0.073
<i>bphA</i>	biphenyl dioxygenase	Biphenyl	43	<i>Myxococcus</i>	0.026	0.022	0.038	0.031		0.029	0.031	0.031	0.043	0.023
<i>bphC</i>	dihydroxybiphenyl dioxygenase	Biphenyl	10	<i>Rhodococcus</i>					0.028					
<i>carA</i>	carbazole dioxygenase	Carbazole	5	<i>Alcanivorax;</i> <i>Frankia;</i> <i>Marinobacter;</i> <i>Mycobacterium;</i> <i>Pseudomonas</i>	0.011	0.008	0.054	0.025			0.024	0.028		0.021
<i>catB</i>	muconate cycloisomerase	Xylene	42	<i>Bacteroides</i>	0.064	0.081			0.014		0.09			
<i>Catechol</i>	catechol dioxygenase	Xylene	63	<i>Pseudomonas</i>	0.023	0.024	0.097	0.061			0.03			0.085
<i>cbdA</i>	ortho-halobenzoate dioxygenase	2-Chlorobenzoate	6	<i>Burkholderia</i>	0.004	0.006	0.033	0.021		0.005	0.004	0.015	0.02	0.005
<i>ChnE</i>	oxohexanoate dehydrogenase	Cyclohexane	1	<i>Rhodococcus</i>	0.016	0.009		0.06			0.019	0.055		0.037
<i>cmtAb</i>	p-cumate dioxygenase	Cymene	1	<i>Pseudomonas</i>	0.024	0.031	0.043	0.057			0.025	0.054	0.09	0.033
<i>dhph</i>	dihydroxypyridine hydroxylase	Nicotine	1	<i>Arthrobacter</i>			0.045	0.046		0.03	0.08	0.057	0.035	0.067
<i>GCoADH</i>	glutaryl-CoA dehydrogenase	Benzoate	30	<i>Mycobacterium</i>	0.021	0.012	0.081	0.056			0.013	0.084		0.049
<i>mdlA</i>	mandelate racemase	Mandelate	29	<i>Burkholderia</i>	0.023	0.023				0.091	0.034	0.035		0.039
<i>mdlB</i>	mandelate dehydrogenase	Mandelate	4	<i>Actinoplanes;</i> <i>Deinococcus;</i> <i>Delftia;</i> <i>Photorhabdus</i> <i>Klebsiella</i>	0.04	0.057					0.076			
<i>mhpB</i>	3-(2,3-dihydroxyphenyl)propionate 1,2-dioxygenase	Phenylpropionate	1	<i>Klebsiella;</i> <i>Mycobacterium</i>	0.03	0.032	0.046	0.038			0.02	0.082		0.039
<i>mhpC</i>	2-hydroxy-6-keonona-2,4-dienedioic acid hydrolase	Phenylpropionate	2	<i>Klebsiella;</i> <i>Mycobacterium</i>	0.015	0.005	0.072	0.042	0.058		0.009	0.013		0.011
<i>mhqA</i>	hydroquinone 1,2-dioxygenase	Nitrophenol	1	<i>Burkholderia</i>					0.025					
<i>nicdehydr</i>	nicotine dehydrogenase	Nicotine	1	<i>Mycobacterium</i>					0.016					
<i>nitA</i>	nitrilase	Phenylacetaldoxime	41	<i>Burkholderia</i>	0.025	0.021					0.035			
<i>ohbAB</i>	halobenzoate dioxygenase	Benzoate	11	<i>Ralstonia</i>	0.015	0.01		0.087		0.058	0.011	0.027		0.033
<i>pcaG</i>	protocatechuate 3,4-dioxygenase	Protocatechuate	31	<i>Bordetella</i>	0.013	0.022	0.012	0.017		0.051	0.015	0.021	0.008	0.019
<i>phdCI</i>	carboxylate isomerase	Nphthalene	5	<i>Burkholderia;</i> <i>Cupriavidus;</i> <i>Erythrobacter;</i> <i>Xanthobacter</i> <i>Nocardioides</i>	0.048	0.034	0.072	0.049		0.016	0.038	0.047	0.037	0.037
<i>phdK</i>	carboxybenzaldehyde dehydrogenase	Phenanthrene	1		0.038	0.045					0.058	0.065		0.061
<i>PobA</i>	hydroxybenzoate hydroxylase	phenoxybenzoate	17	<i>Sinorhizobium</i>	0.001	0.001	0.01	0.003		0.001	0.001	0.002	0.004	0.002
<i>ofdA</i>	2,4-D/alpha-ketoglutarate dioxygenase	Dichlorophenoxyacetic Acid	39	<i>Caulobacter;</i> <i>Cupriavidus;</i> <i>Mycobacterium</i>					0.01					
<i>tomA</i>	toluene monoxygenase	Toluene	1	<i>Verminephrobacter</i>	0.002	0.004	0.048	0.026		0.019	0.006	0.01	0.019	0.008

Table S7. MC-252 alkane half-life (days) from field and laboratory with currents that would allow 2 days or 5 days to move 10 km from source. According to Camilli et al () the plume is constrained by bathymetric features but the width of plume can double over the distance of our study area, our data also indicates that the vertical extent of the plume varies from 100 m at the source to 200 m at locations distant from the plume. Based on this information the plume has a relatively stable configuration but conservatively could expect dilution alone to represent up to half of the reported half-life in the plume data. Lab simulations suggest that these decay rate estimates are reasonable.

		plume	plume	BP data	BP data	Mixed	Microcosm
		samples (2 d)	samples (5 d)	(2 d)	(5 d)	Consortia, 5°C	water, 5°C
	Average	2.4	6.1	1.2	2.9	3.5	2.2
n-Tridecane	C13alk	1.6	4	1.4	3.5	3.1	2.1
n-Tetradecane	C14alk	1.5	3.8	1.4	3.4	3.5	2.3
Pentadecane	C15alk	1.5	3.8	1	2.4	3.6	2.1
n-hexadecane	C16alk	1.6	4	2	5	3.6	2.2
n-							
heptadecane	C17alk	1.7	4.3	1.1	2.8	3.6	2.3
Pristane	C19teralk	1.6	4.1	1.3	3.2	3	2.3
n-octadecane	C18alk	2.1	5.2	1	2.6	4.2	2.3
Phytane	C20teralk	1.8	4.6	1.4	3.4	3.6	2.3
n-Nonadecane	C19alk	2.1	5.4	1	2.6	3.6	2.3
eicosane	C20alk	3.2	7.9	1	2.5	3.7	2.3
Heneicosane	C21alk	3.7	9.3	1.9	4.7	3.5	2.6
n-Docosane	C22alk	3.8	9.5	1	2.5	3.7	2.2
tricosane	C23alk	3.7	9.2	1	2.5	3.6	2.2
tetracosane	C24alk	3.2	8	0.9	2.2	3.5	2.3
n-Pentacosane	C25alk	2.8	7	0.8	1.9	3.6	2
n-hexacosane	C26alk	3.1	7.8	0.6	1.6	3.1	1.7

Table S8. Twenty-six 16S rDNA mixtures from different species were prepared as mock communities using a semi-randomized latin square structure. A stepwise function was used so that each successive organism was added at final a concentration 37% greater than the previous organism. Each test organism was represented in all mixtures at each possible concentration step.

Initial Mass (ng)	Final Conc. (pM)	Latin Square PhyloChip																										
		1	2	3	4	5	6	7	8	9	10	11	12	13	14	15	16	17	18	19	20	21	22	23	24	25	26	
0.00	0.00	A	I	Z	W	O	F	X	B	N	E	D	R	L	G	Q	U	C	K	M	E	V	Y	H	P	J	T	S
0.03	0.25	Y	L	R	U	T	H	D	Z	W	X	S	J	B	C	F	V	K	M	E	Q	G	I	N	P	J	O	A
0.05	0.34	X	O	B	Y	P	S	U	A	G	J	Z	E	C	F	H	D	N	I	K	W	Q	R	V	L	M	T	E
0.06	0.47	J	H	P	S	A	X	Y	K	L	Z	M	N	I	O	R	Q	V	D	F	T	B	C	W	G	U	E	P
0.09	0.64	G	B	E	Q	R	T	Z	F	H	Y	O	C	J	X	V	M	L	U	N	S	K	A	I	W	D	P	I
0.12	0.88	C	J	Q	F	K	O	H	V	U	D	T	G	R	A	Y	B	E	P	Z	L	N	X	S	M	W	I	H
0.17	1.21	N	K	D	O	F	U	P	S	A	B	W	V	G	Z	M	L	X	Q	T	E	C	J	Y	R	I	H	U
0.23	1.65	H	G	I	C	E	A	K	R	J	Q	L	O	N	S	B	W	Z	X	D	Y	F	V	M	T	P	U	V
0.31	2.26	W	M	S	A	D	Z	T	U	Q	R	X	B	P	E	O	F	G	Y	I	J	H	N	K	C	L	V	X
0.43	3.10	Q	E	K	L	G	B	M	W	S	P	C	U	Y	T	J	A	F	H	R	D	I	Z	O	N	V	X	W
0.58	4.25	P	U	Y	R	N	E	L	C	D	F	A	M	T	Q	G	I	H	J	V	O	Z	K	B	X	S	W	Z
0.80	5.82	T	C	V	M	H	G	Q	D	O	N	U	X	E	R	W	P	B	A	L	I	S	F	J	K	Y	Z	B
1.10	7.98	M	T	N	Z	J	K	A	L	F	G	P	H	S	I	X	R	Y	W	U	C	V	E	D	O	Q	B	L
1.50	10.93	O	V	X	N	M	D	I	E	T	U	K	Q	W	Y	P	S	R	C	J	B	A	G	H	F	Z	L	O
2.06	14.97	L	S	T	H	I	C	W	Y	R	V	E	Z	D	J	K	X	U	N	P	G	M	Q	F	B	A	L	M
2.82	20.51	Z	R	A	E	B	V	S	X	K	I	Q	L	U	N	D	Y	W	G	O	F	P	T	C	H	J	M	J
3.86	28.10	B	X	C	K	L	Y	R	N	P	S	F	I	Z	H	T	O	M	V	W	U	E	D	Q	A	G	J	J
5.29	38.50	S	Y	H	I	X	W	J	O	B	M	G	D	V	K	Z	E	P	L	C	R	T	U	A	Q	N	F	C
7.24	52.75	E	D	F	V	Q	P	N	G	Z	A	B	W	O	U	I	J	T	R	Y	H	X	M	L	S	K	C	R
9.92	72.26	K	Z	G	X	Y	M	E	J	I	L	V	F	H	P	C	T	A	S	Q	N	O	W	U	D	B	R	K
13.59	99.00	R	Q	M	D	C	I	B	P	V	W	H	S	F	L	N	Z	J	T	X	A	U	O	G	Y	E	K	Y
18.62	135.63	D	F	J	T	U	L	G	I	M	C	N	P	Q	V	A	K	O	B	H	Z	W	S	X	E	R	Y	N
25.51	185.81	U	P	O	B	Z	Q	V	H	C	K	R	Y	M	W	S	G	D	E	A	X	J	L	T	I	F	N	Q
34.95	254.56	V	W	L	P	S	J	F	T	X	H	Y	A	K	D	E	N	I	O	G	M	R	B	Z	U	C	H	G
47.88	348.75	F	A	U	J	W	N	O	M	E	T	I	K	X	B	L	C	Q	Z	S	P	D	Y	R	V	H	Q	D
65.59	477.79	I	N	W	G	V	R	C	Q	Y	O	J	T	A	M	U	H	S	F	B	K	L	P	E	Z	X	X	D

Legend

A	<i>Pseudomonas aeruginosa</i>	I	<i>Bacillus anthracis</i>	Q	<i>Dechloromonas agitata</i>	Y	<i>Sulfolobus solfataricus</i>
B	<i>Dechloromonas aromatica</i>	J	<i>Desulforudis sp.</i>	R	<i>Ralstonia pickettii</i>	Z	<i>Methanocaldococcus jannaschii</i>
C	<i>Caulobacter crescentus</i>	K	<i>Staphylococcus warneri</i>	S	<i>Desulfovibrio vulgaris</i>		
D	<i>Francisella tularensis</i>	L	<i>Geothrix fermentans</i>	T	<i>Geobacter sulfurreducens</i>		
E	<i>Dehalococcoides ethenogenes</i>	M	<i>Arthobacter oxydans</i>	U	<i>Borrelia burgdorferi</i>		
F	<i>Geobacter metallireducens</i>	N	<i>Bacteriodes fragilis</i>	V	<i>Deinococcus radiodurans</i>		
G	<i>Campylobacter jejuni</i>	O	<i>Prevotella melaninogenica</i>	W	<i>Thermotoga maritima</i>		
H	<i>Nostoc sp.</i>	P	<i>Xanthobacter autotrophicus</i>	X	<i>Helicobacter pylori</i>		

Figures

Figure S1. Sampling sites around the MC252 well head from May 25 to June 2, 2010.

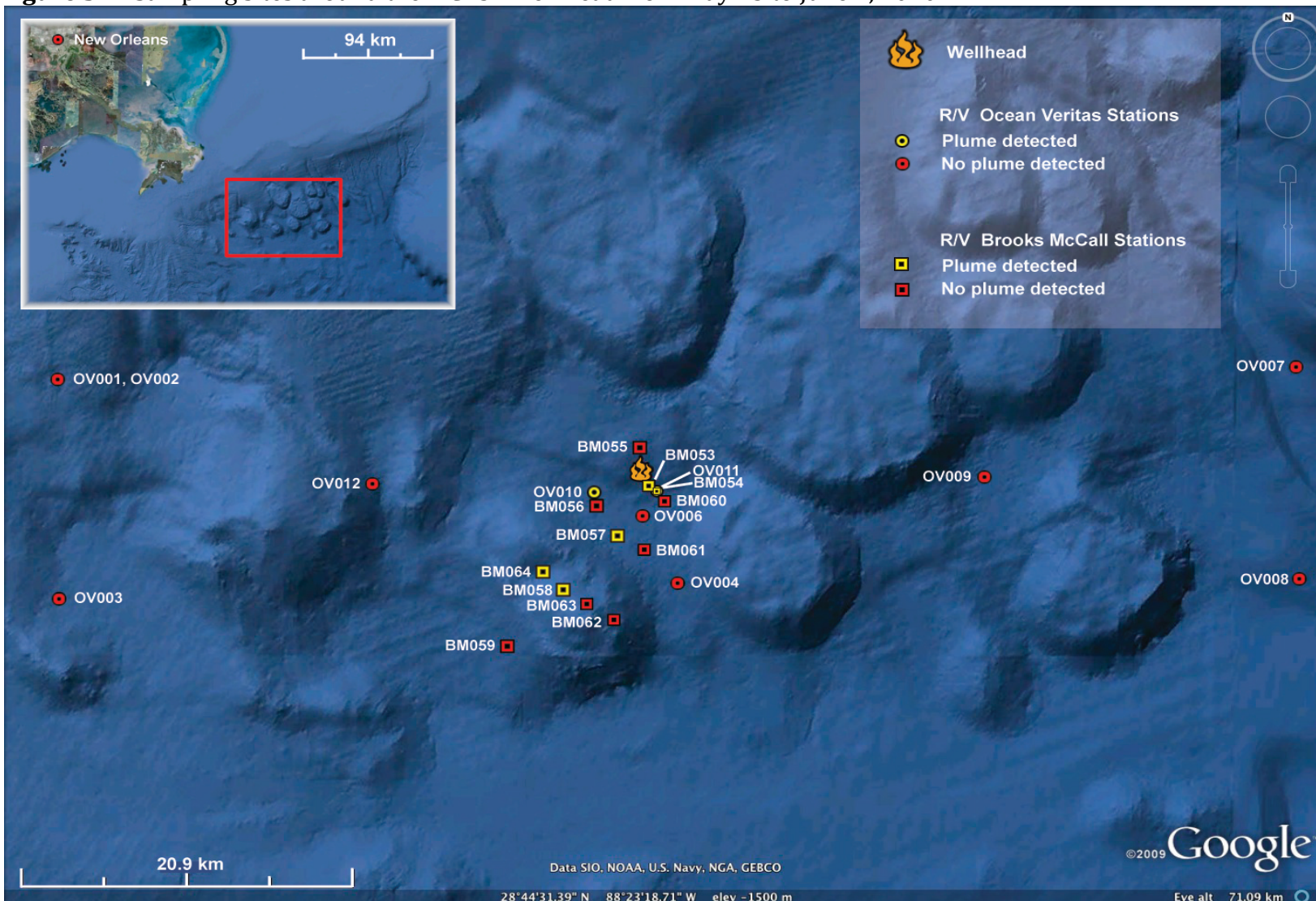


Figure S2. Measured water concentrations of total BTEX, alkanes, and PAH concentrations by depth and distance from the MC252 well head from May 9, 2010 until June 19, 2010.

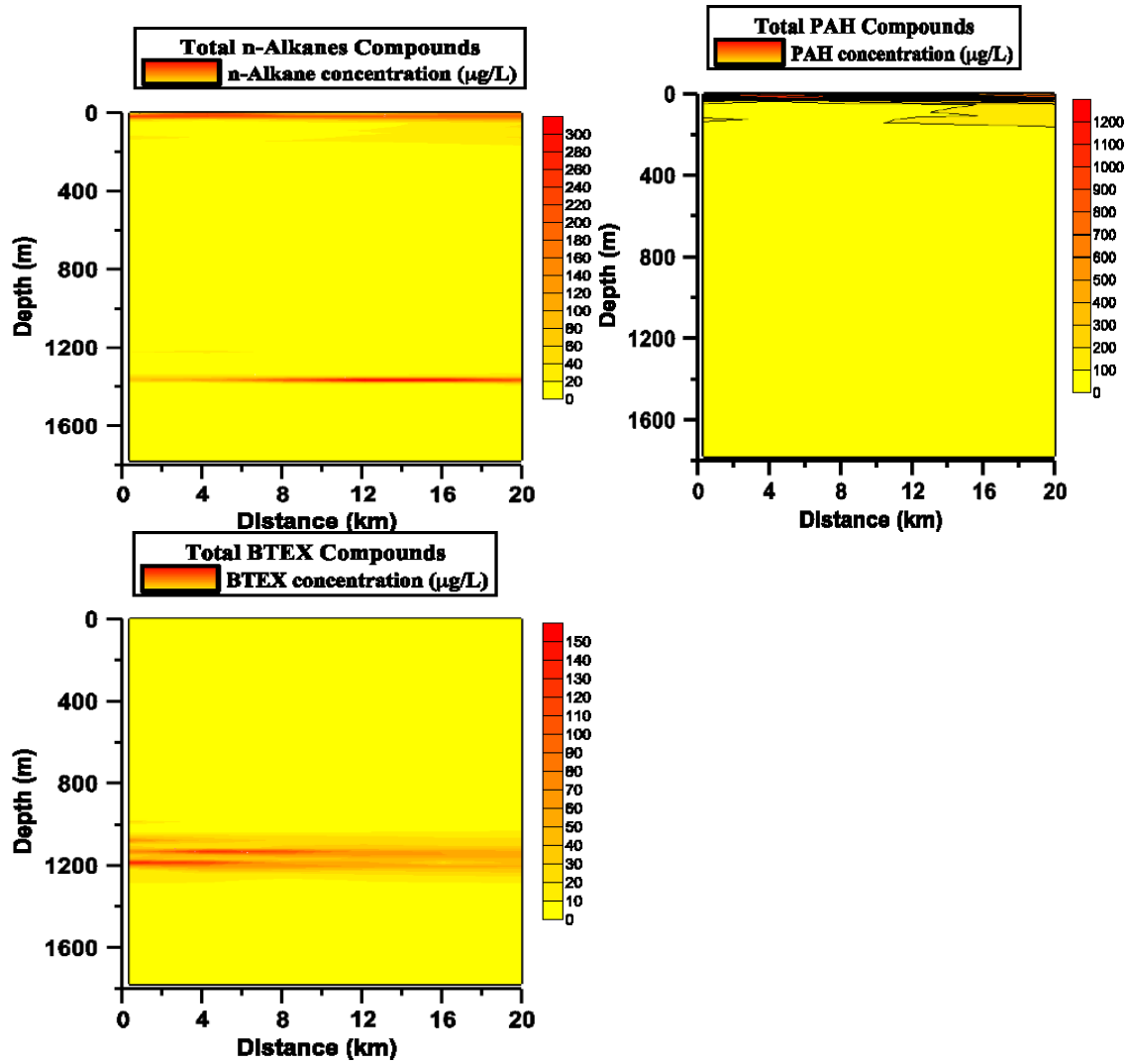
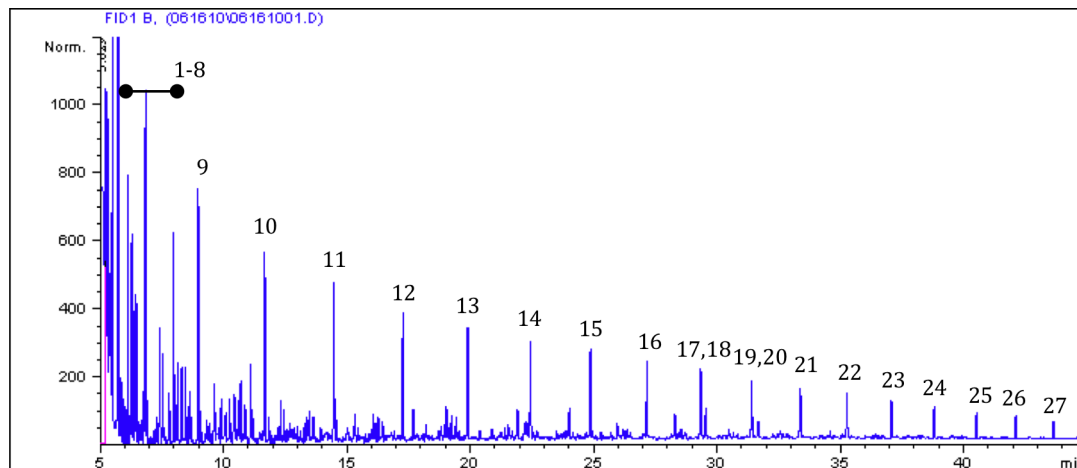


Figure S3. Chromatogram for MC252 oil from the wellhead.



Pk#	FID RT (min)	ID
1	6.3	heptane
2	6.4	methylcyclohexane
3	6.5	ethylcyclopentane
4	6.5	cyclopentane, 1,2,4 trimethyl
5	6.7	cyclopentane, 1,2,3 trimethyl
6	6.8	toluene
7	6.9	2 methyl heptane
8	8.1	n-octane
9	9.0	n-Nonane
10	11.7	n-Decane
11	14.5	n-Undecane
12	17.3	n-Dodecane
13	19.9	n-Tridecane
14	22.5	n-Tetradecane
15	24.9	Pentadecane
16	27.2	n-hexadecane
17	28.6	n-Undecane
18	29.4	Pentadecane, 2,6,10,14-tetramethyl
19	31.5	n-octadecane
20	31.7	Hexadecane, 2,6,10,14-tetramethyl-
21	33.4	n-Nonadecane
22	35.3	eicosane
23	37.1	Heneicosane
24	38.8	n-Docosane
25	40.5	tricosane
26	42.1	tetracosane
27	43.6	n-Pentacosane

Figure S4. Bacterial richness detected in oil plume. A total of 951 subfamilies were detected in 62 bacterial phyla using Phylogenetic microarray (PhyloChip) analysis (see supplemental methods). Only 16 subfamilies in one subphylum (γ -proteobacteria) were significantly enriched in the plume relative to outside the plume.

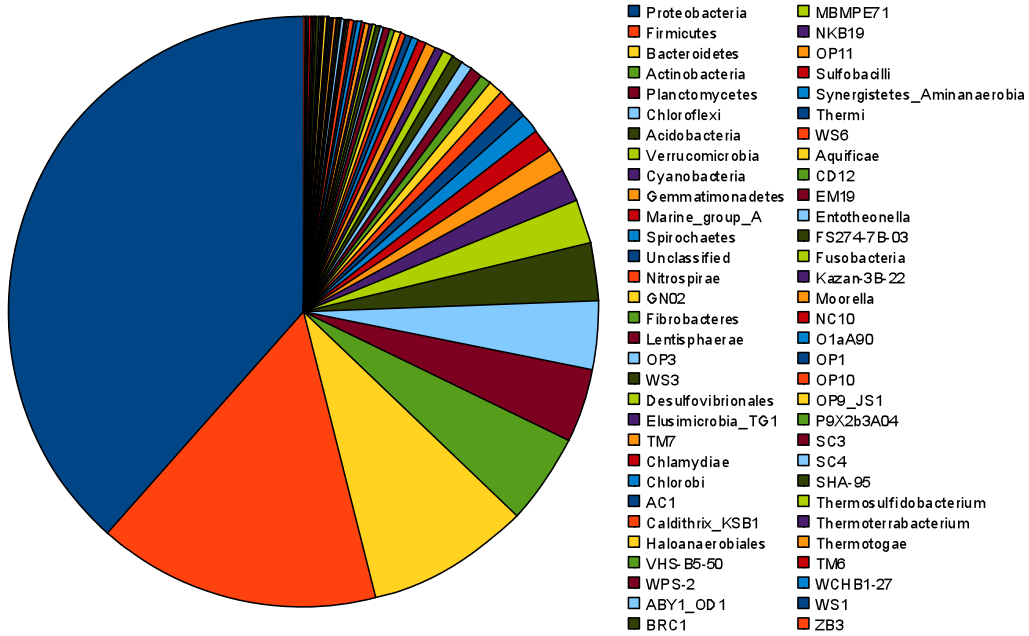


Figure S5. Bacterial taxa enriched by oil plume. Differences in estimated 16S rRNA gene concentration are shown as percent of non-plume concentration for a representative OTU in each of the 16 subfamilies that were significantly enriched in plume samples (Table S2).

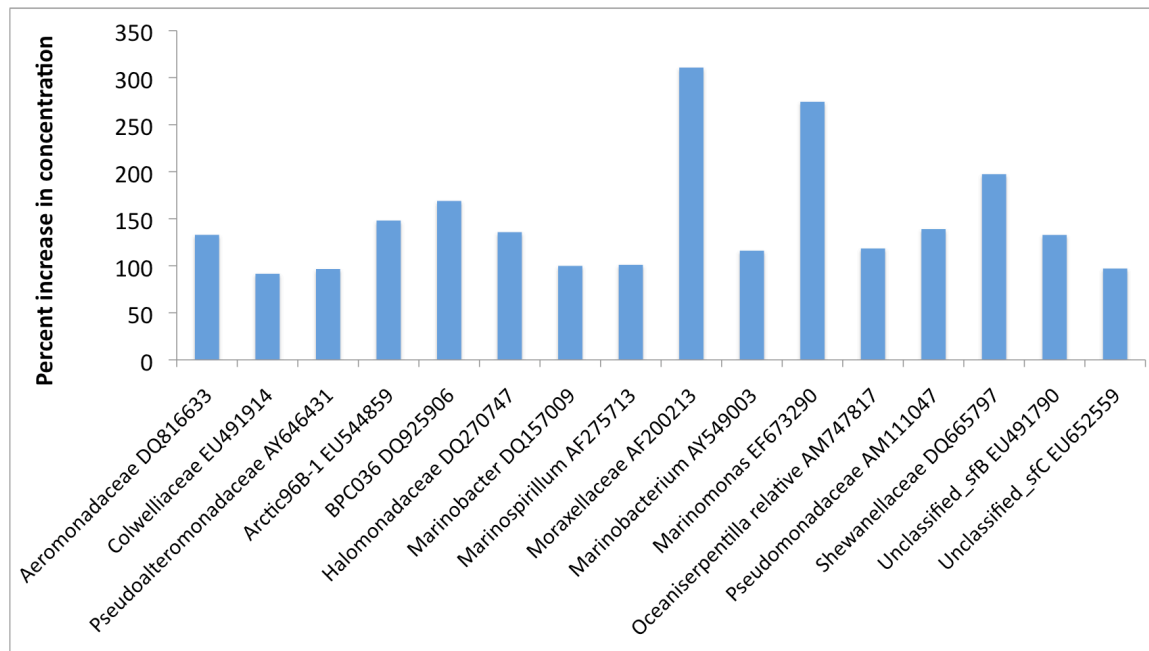


Figure S6. Correspondence analysis of alkanes with distance from the plume, fluorometry data, and AODC cell counts.

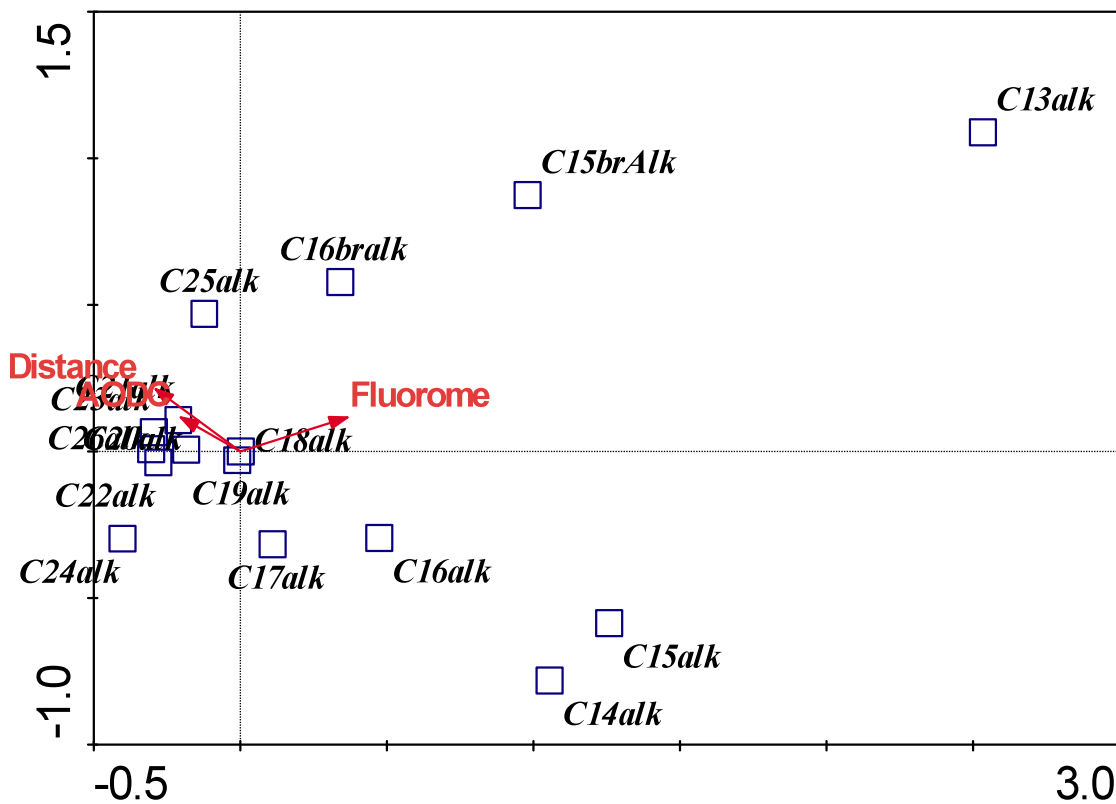


Figure S7. DCA analysis of the normalized signal intensity data for oil-contaminated samples and non-oil samples showing that the oil spill significantly affected the microbial community structure. The signal intensity of the functional gene sequences present in at least two of 5 samples were used for DCA. The filled circles are for oil-contaminated samples, and non-filled circles are for non-oil samples.

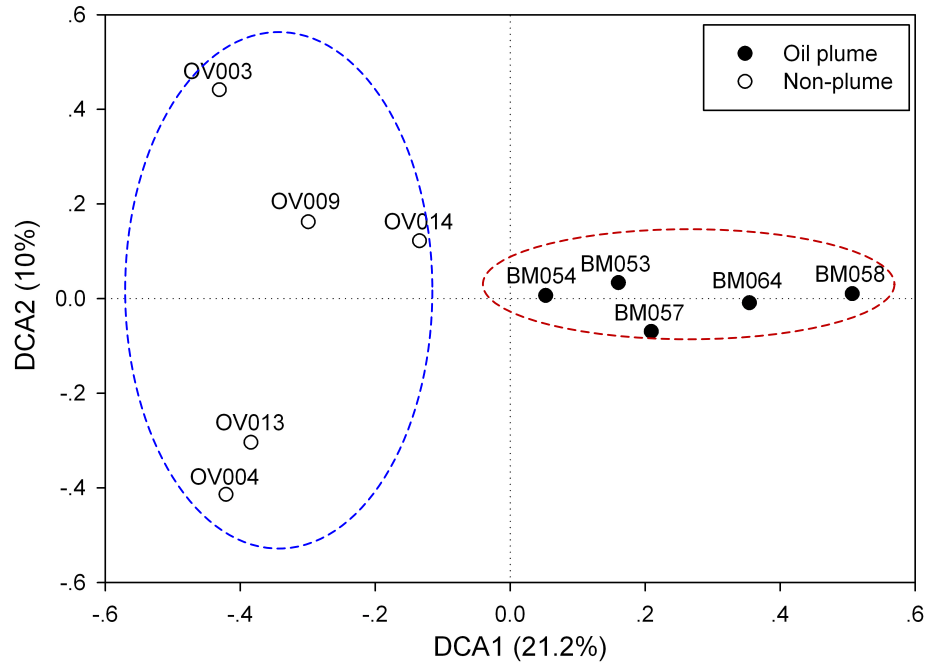


Figure S8. The normalized total signal intensity of the detected genes involved in alkanes, alkynes, cycloalkanes and aromatic carboxylic acid degradation. The normalized signal intensity for each functional gene was the average of the total signal intensity of all detected genes from all the replicates. All data are presented as mean \pm SE. ** $p < 0.01$, * $p < 0.05$. It should be noticed that Hydrocarbon degradation genes: *alkB*, alkane 1-monooxygenase; *alkH*, aldehyde dehydrogenase; *alkJ*, alcohol dehydrogenase; *BMO*, butane monooxygenase; *ChnA*, cyclohexanol dehydrogenase; *chnB*, cyclohexanone 1,2-monooxygenase; *ChnE*, 6-oxohexanoate dehydrogenase; *cpnB*, cyclopentanone 1,2-monooxygenase; *Xamo*, alkene monooxygenase. Aromatic carboxylic acid degradation genes: *bclA*, benzoate-CoA ligase; *bco*, benzoyl CoA reductase; *benAB*, benzoate 1,2-dioxygenase; *benD*, benzoate/cis-diol dehydrogenase; *BpH*, benzoate 4-monooxygenase; *GcdB*, glutaconyl-CoA/decarboxylase; *GCoADH*, glutaryl-CoA dehydrogenase; *HcaB*, 2,3-dihydroxy-2,3-dihydrophenylpropionate/ dehydrogenase; *hmgA*, homogentisate 1,2-dioxygenase; *hmgB*, fumarylacetoacetase; *hmgC*, maleylacetoacetate isomerase; *mdlA*, mandelate/racemase; *mdlB*, L-mandelate dehydrogenase; *mdlC*, benzoylformate decarboxylase; *mhpA*, 3-(3-hydroxyphenyl)propionate hydroxylase; *nagG*, salicylate 5-hydroxylase; *nagI*, gentisate 1,2-dioxygenase; *nagK*, acylpyruvate/hydrolase; *nagL*, maleylpyruvate isomerase; *ohbAB*, halobenzoate 1,2-dioxygenase; *ophC*, 4,5-dihydroxyphthalate/decarboxylase; *PhaB*, acetoacetyl-CoA reductase; *phtA*, phthalate 4,5-dioxygenase; *pimF*, enoyl-CoA hydratase; *PobA*, p-hydroxybenzoate hydroxylase; *xylG*, 2-hydroxymuconic semialdehyde dehydrogenase.

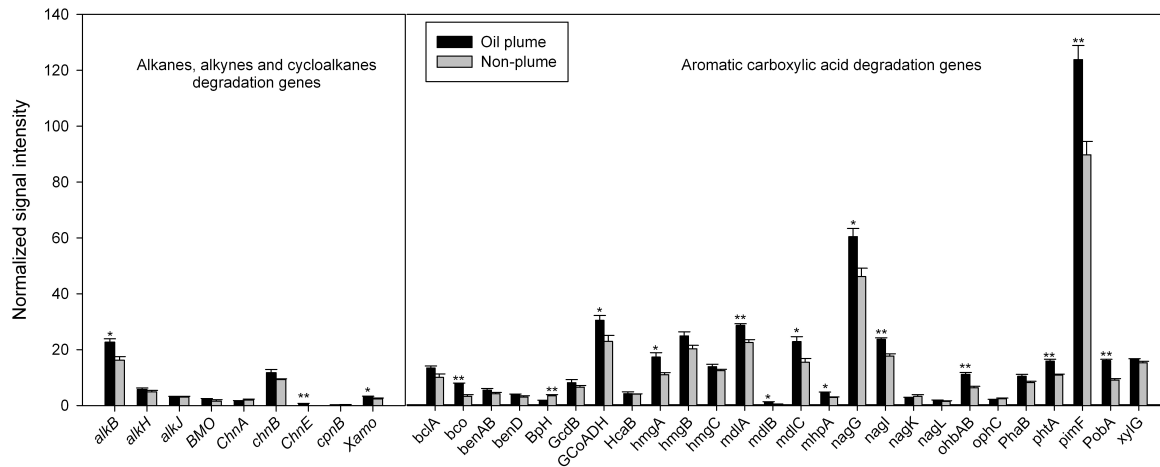


Figure S9. The normalized total signal intensity of the detected genes involved in other aromatics (except aromatic carboxylic acid). The normalized signal intensity for each functional gene was the average of the total signal intensity of all detected genes from all the replicates. All data are presented as mean \pm SE. ** $p < 0.01$, * $p < 0.05$. A, BTEX and related aromatics; B, chlorinated aromatics; C, heterocyclic aromatics; D, nitroaromatics; E, other aromatics; F, polycyclic aromatics. *akbF*, 4-hydroxy-2-oxovalerate aldolase; *Apc*, acetophenone carboxylase; *bbs*, E-phenylitaconyl-CoA hydratase; *catB*, muconate cycloisomerase; *pchCF*, 4-cresol dehydrogenase; *todC*, toluene dioxygenase; *tutFDG*, benzylsuccinate synthase; *xyIC*, benzaldehyde dehydrogenase; *cbdA*, ortho-halobenzoate dioxygenase; *tfdA*, 2,4-D/alpha-ketoglutarate dioxygenase; *tfdB*, chlorophenol monooxygenase; *tftH*, hydroxyquinol 1,2-dioxygenase; *arhA*, PAH dioxygenase; *carA*, carbazole dioxygenase; *nbaC*, 3-hydroxyanthranilate 3,4-dioxygenase; *nhh*, nitrile hydratase; *nmoA*, nitrilotriacetate monooxygenase; *pnbA*, nitrobenzoate nitroreductase; *AmiE*, aliphatic amidase; *Arylest*, arylesterase/ aryl-ester hydrolase/ aromatic esterase; *BADH*, benzylalcohol dehydrogenase; *Catechol*, catechol 1,2-dioxygenase; *catechol_B*, catechol 2,3-dioxygenase; *CDD*, dienolate decarboxylase; *cmuA*, alpha subunit of ethylbenzene dioxygenase; *mdlD*, benzaldehyde dehydrogenase; *nitA*, nitrilase; *pcaG*, protocatechuate 3,4-dioxygenase; *pheA*, phenol 2-monooxygenase; *proO*, protocatechuate 4,5-dioxygenase; *xlnD*, hydroxybenzoate hydroxylase; *bphA*, biphenyl 2,3-dioxygenase; *bphC*, 2,3-dihydroxybiphenyl 1,2-dioxygenase; *bphD*, 2-hydroxy-6-oxo-6-phenylhexa-2,4-dienoate hydrolase; *nahA*, naphthalene 1,2-dioxygenase; *phdCl*, carboxylate/isomerase.

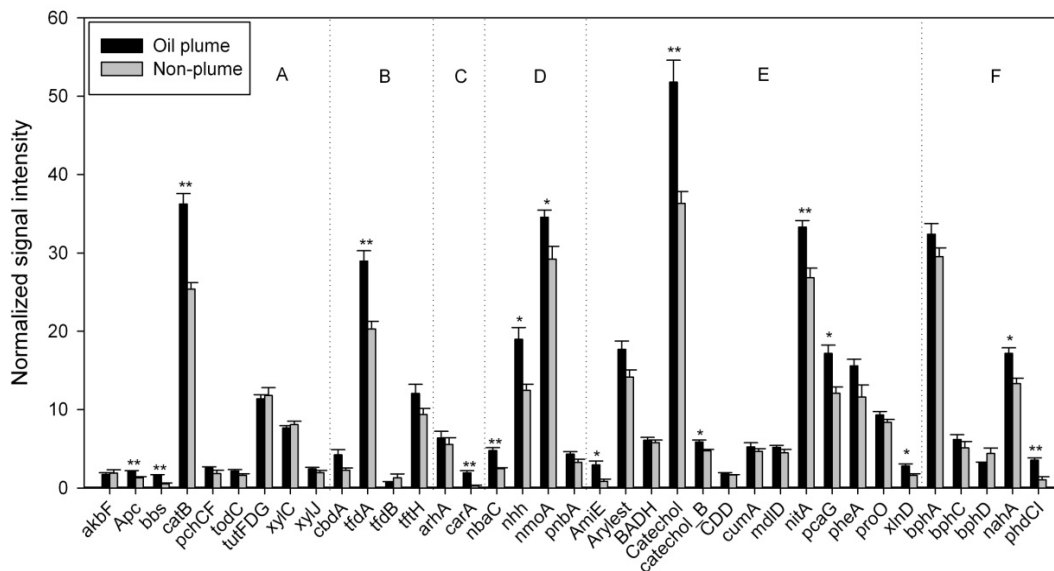


Figure S10. Consortia experiment (no Corexit)- 8day.

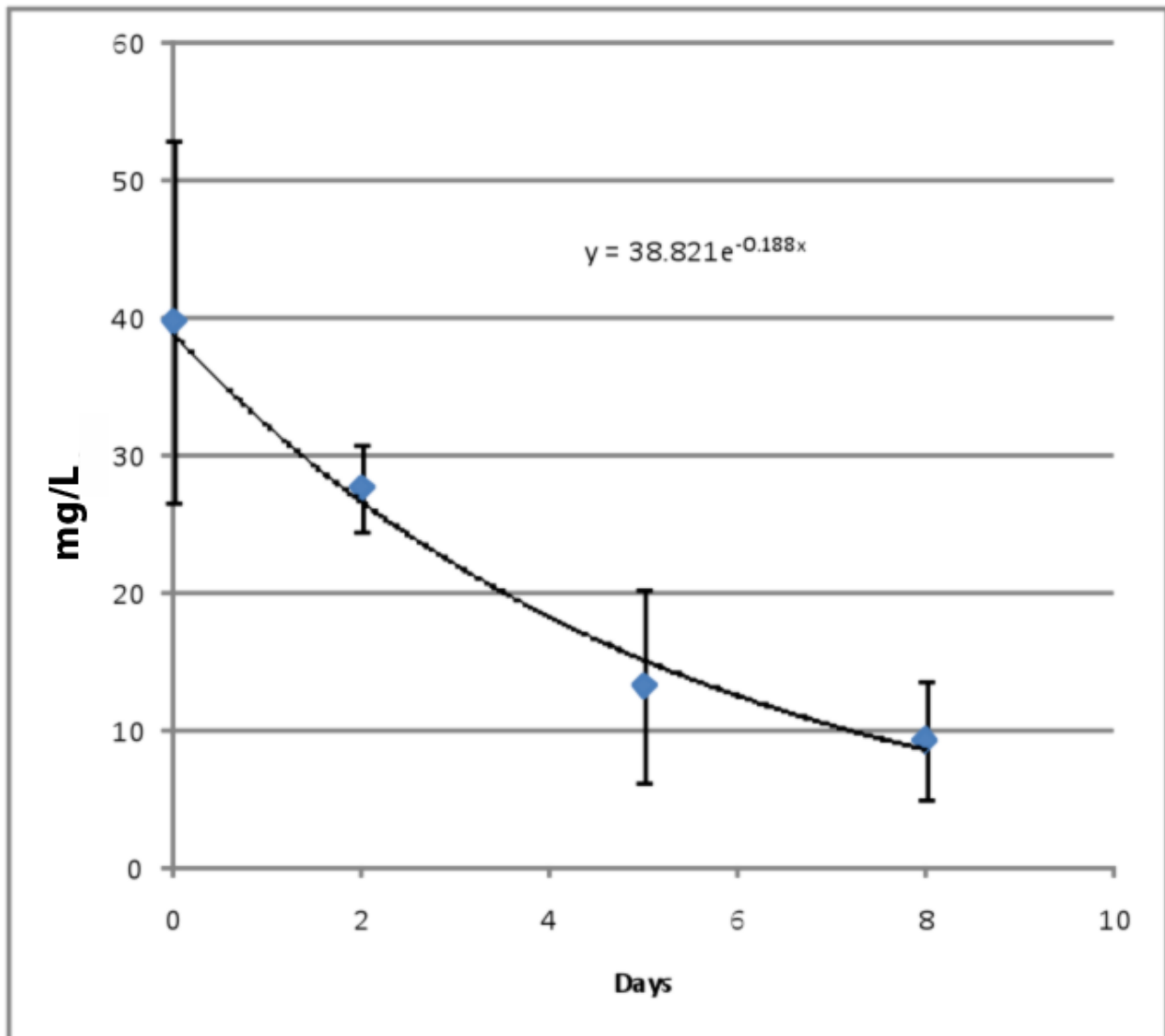


Figure S11. Respirometer 1 without Corexit

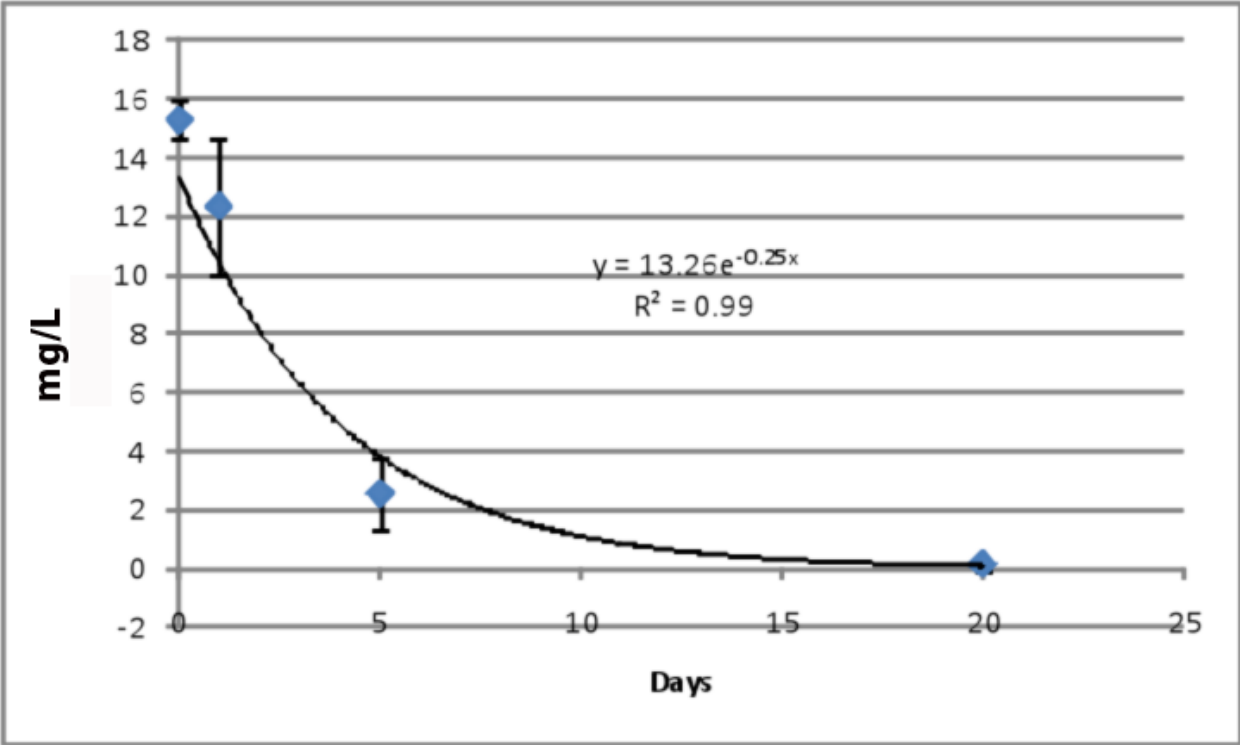


Figure S12. Distribution of mean sequence divergence within OTUs. Sequence differences were determined using the F84 method after NAST alignment (S17) as previously described(S52). The method was chosen due to its recognition by phylogenetic tree reconstruction biologists (S53). The method masks the hypervariable regions resulting in less perceived dissimilarity. The majority of the OTUs contain either singleton genes or sets of genes with no divergence among the conserved positions.

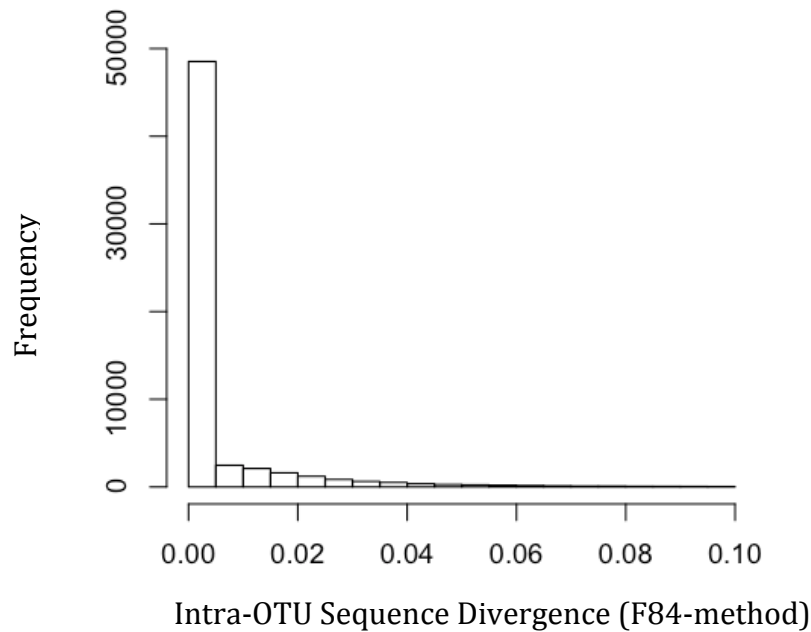
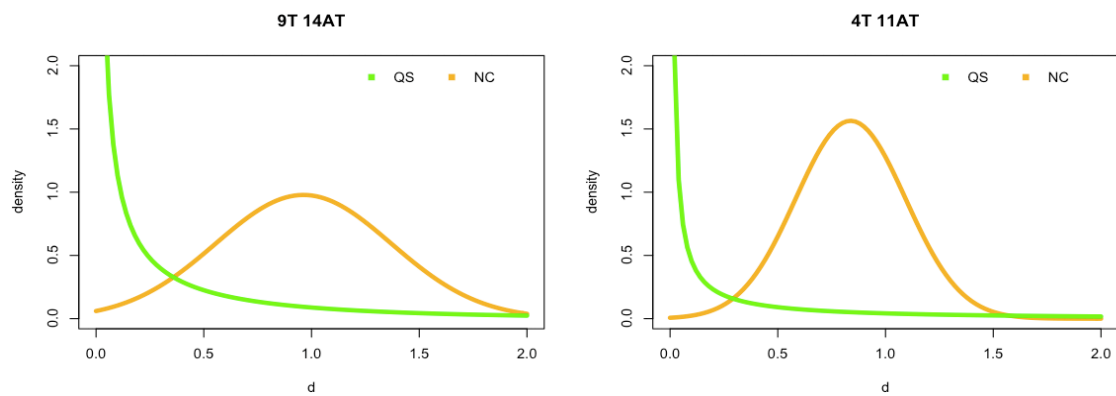


Figure S13. Variation among distribution of pair difference scores, d , between quantitative standards (QS) and negative controls (NC) and between target's AT content.



//

Figure S14. Background-subtracted probe intensities from 12,202 replicate probes representing 3,548 different 25-mer combinations were used to determine the coefficient of variation (CV) for each array. CV grouped by mock community mix where each mix was analyzed in three different hybridizations on different days. Overall the mean CV was 0.097.

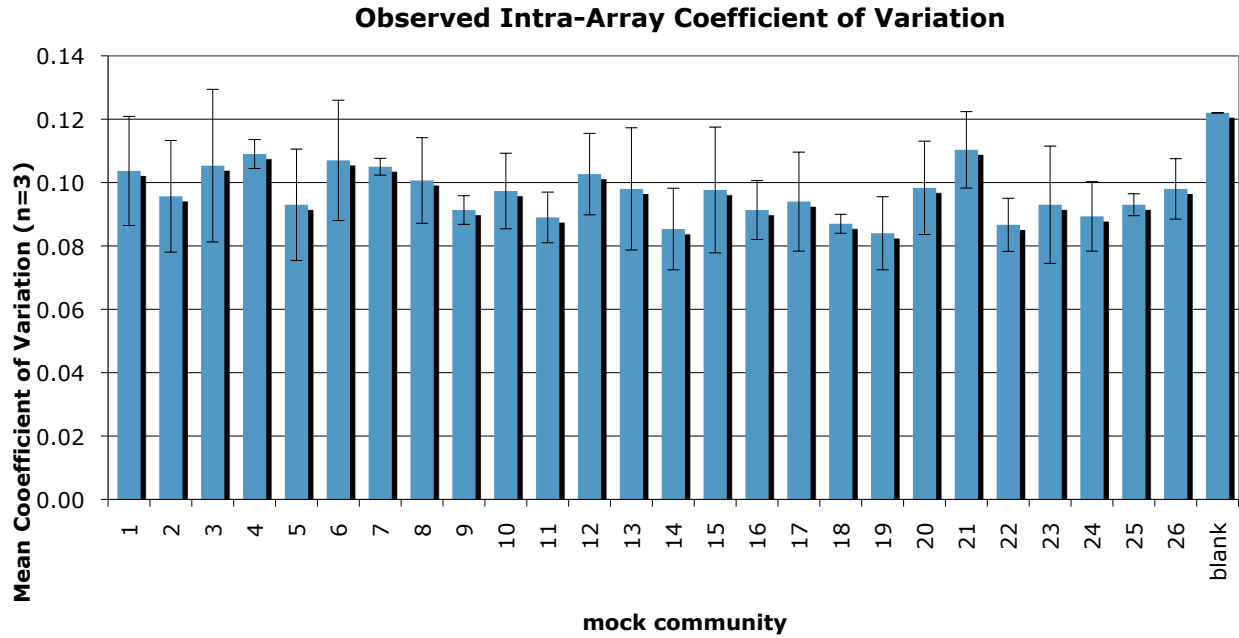


Figure S15. Relationships between HybScore and Concentration. X-axis is \log_2 concentration of the amplicon in the hybridization mixture expressed in picomolar (pM). Y-axis is \log_2 hybridization score (HybScore).

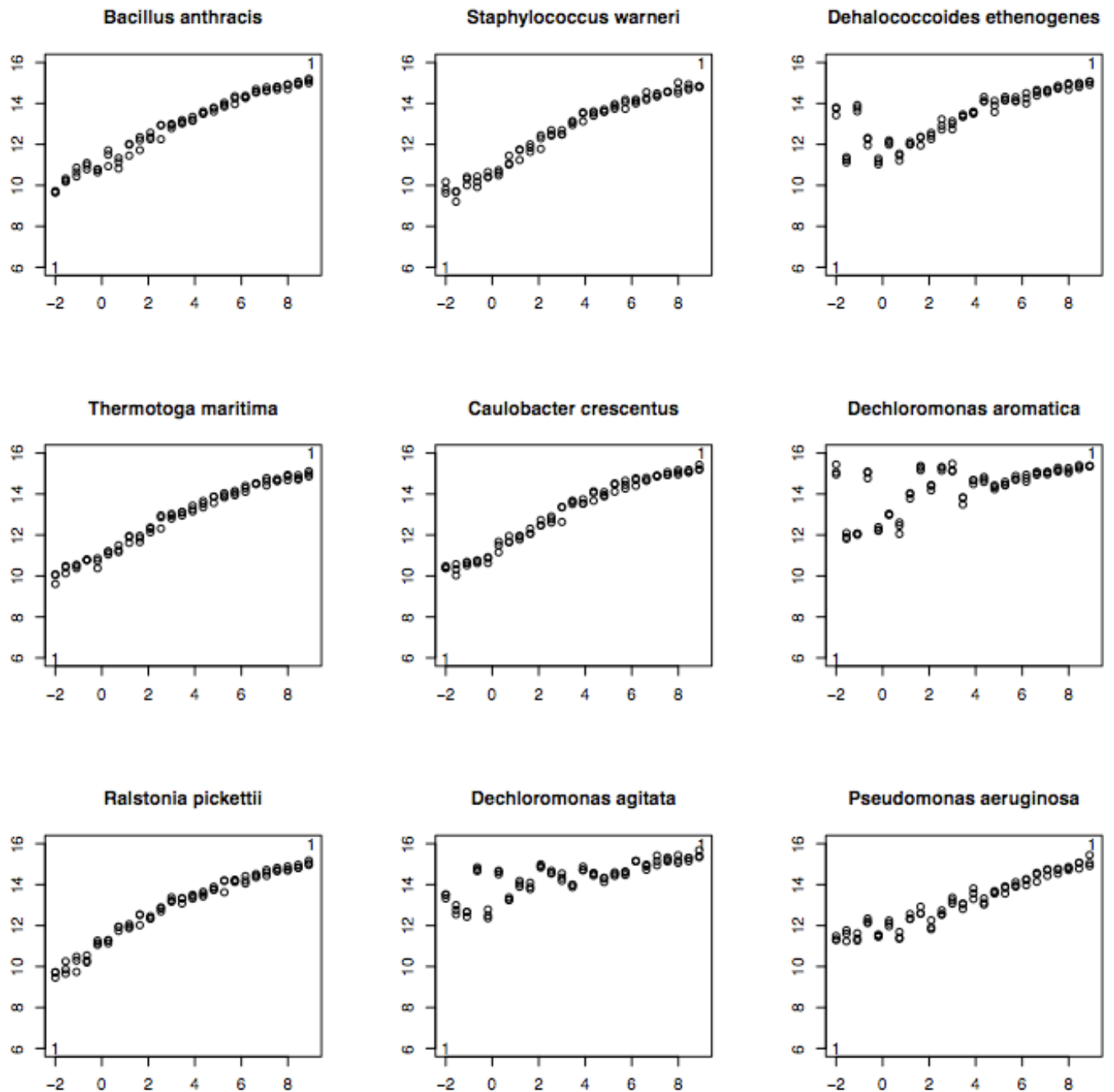


Figure S15 (cont.)

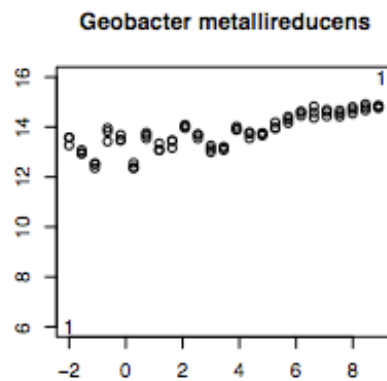
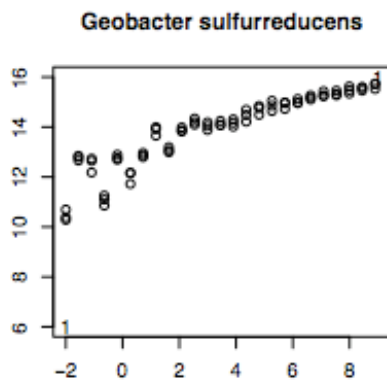
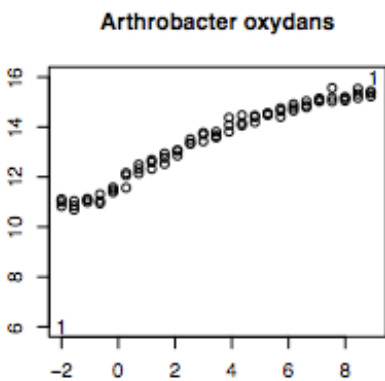
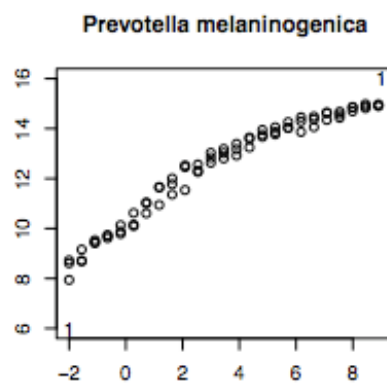
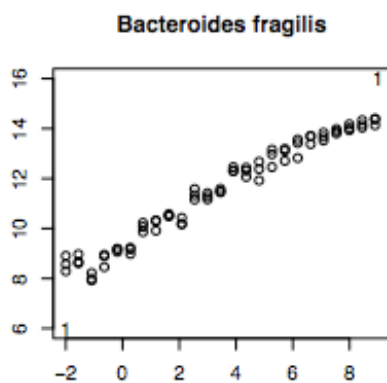
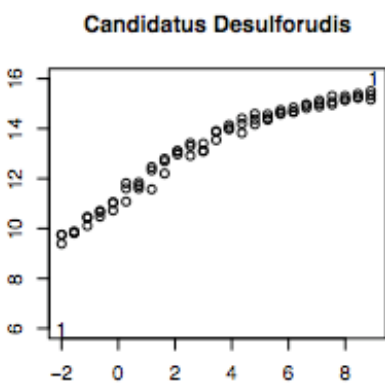
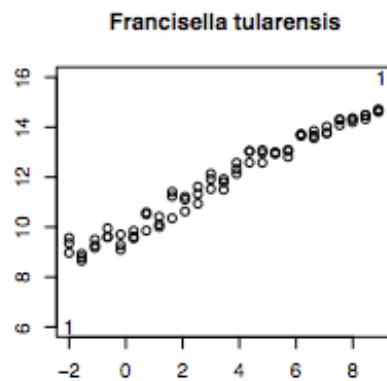
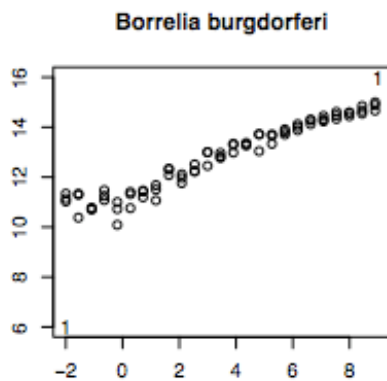
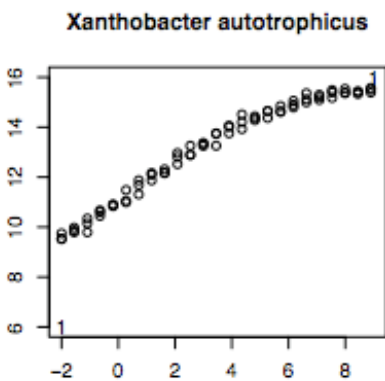


Figure S15 (cont.)

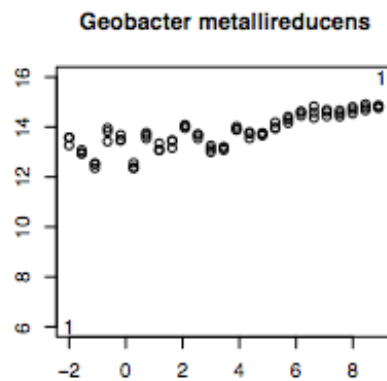
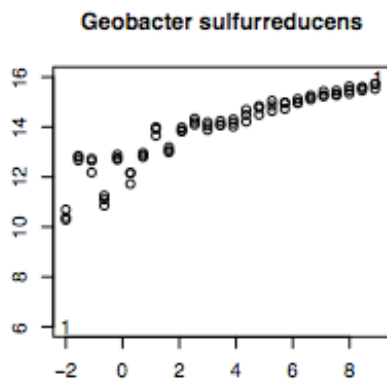
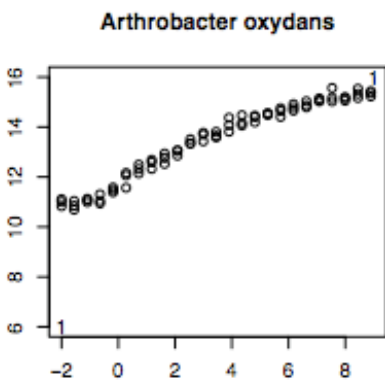
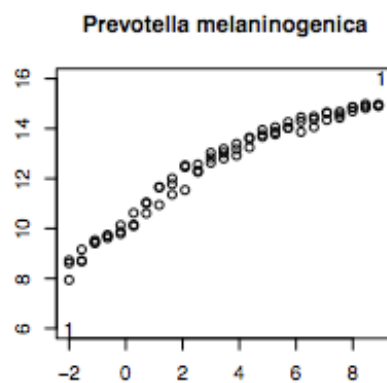
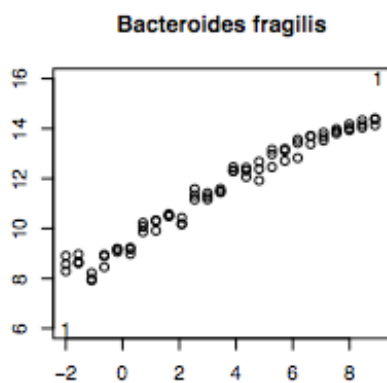
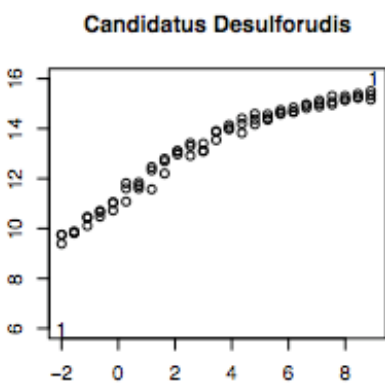
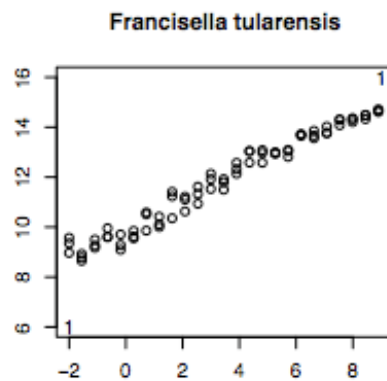
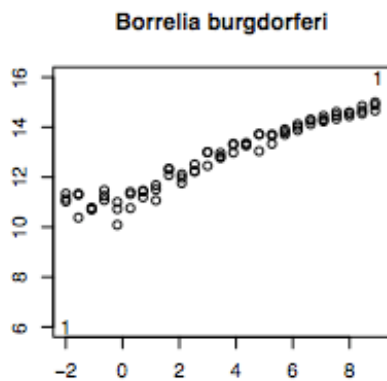
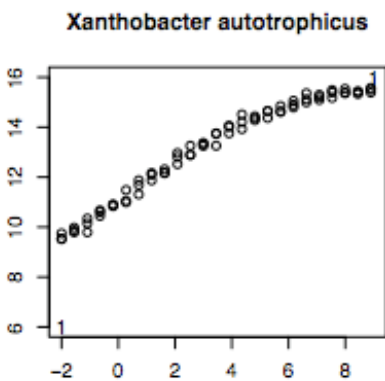


Figure S16. Receiver Operator Characteristic (ROC) curve analysis of Stage 1 P/A. The y-axis, Expected Positive Rate, is the fraction of OTUs expected to be present that were called present. The x-axis, Unexpected Positive Rate, is the fraction of OTUs not-expected to present that were called present. The performance of the rQ_1 , rQ_2 and rQ_3 thresholds are shown in top, center and bottom panels, respectively. Color bar indicates the threshold tested at each point and ranges from the least stringent, 0, to most stringent, 1. Plots were created with rocr, Plots were created with rocr (<http://rocr.bioinf.mpi-sb.mpg.de>)

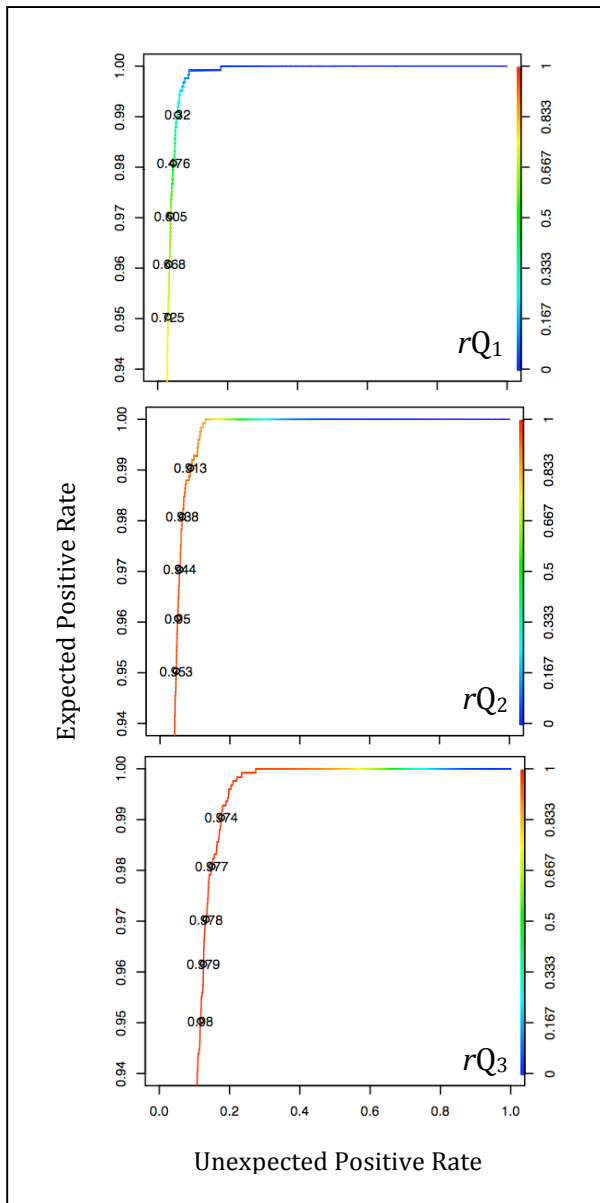


Figure S17. Ordination of 78 Latin Square PhyloChips results. Each of 26 mock communities were replicated 3 three times. Inter-array distance was calculated with either the weighted unfrac or Bray-Curtis method and resulting distance matrices were ordinated with NMDS. Back circles represent individual PhyloChip community profiles and green polygons link replicate communities.

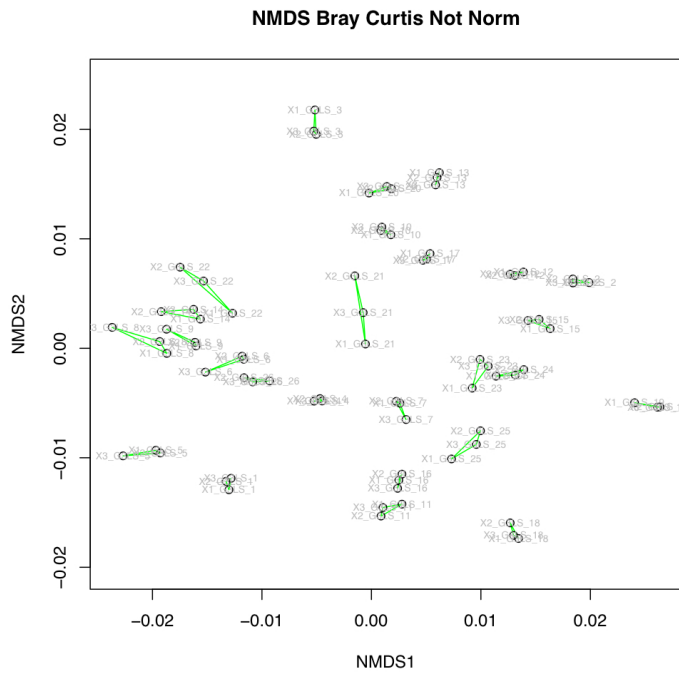
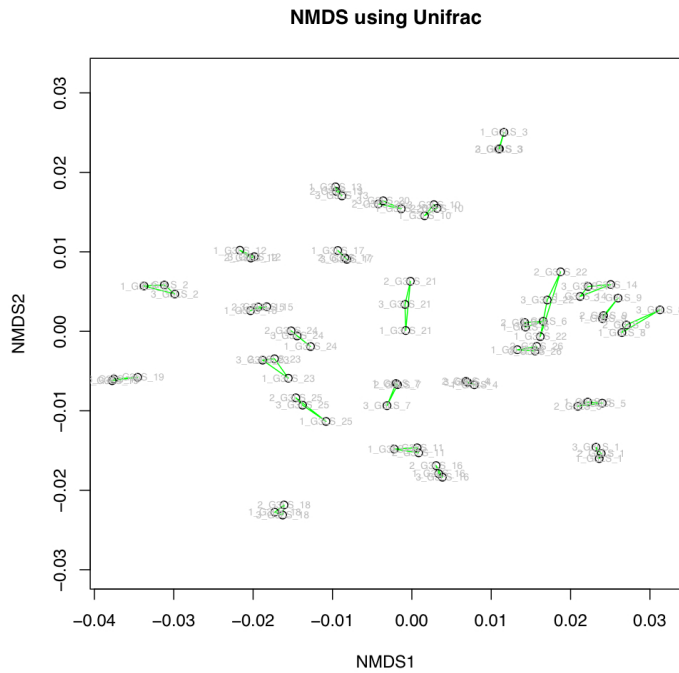


Figure S18. Alkane ratios for sites at various distances from the source indicating changes due to biodegradation, due to lighter hydrocarbons being degraded faster.

